THE EFFECT OF MANGO FIBRES ON STRUCTURAL PROPERTIES OF CONCRETE

NAGEMI PETER

23/U/GMES/0991/PE

A DISSERTATION SUBMITTED TO THE DIRECTORATE OF

RESEARCH AND GRADUATE TRAINING IN PARTIAL

FULFILMENT OF THE REQUIREMENTS FOR THE AWARD OF MASTER OF SCIENCE IN STRUCTURAL ENGINEERING DEGREE

OF KYAMBOGO UNIVERSITY

NOVEMBER 2025

DECLARATION

I **NAGEMI PETER** hereby declare that this submission is my own work and that, to the best of my knowledge and belief. It contains no material previously published or written by another person nor material has been accepted for the award of any degree of the university or other institute of higher learning, except where due acknowledgement has been made in the text and reference list.

Name: NAGEMI PETER

Signature: ……. **Date: ……**

APPROVAL

The undersigned approve that they have read and hereby recommend for submission to the Directorate of Research and Graduate Training of Kyambogo University, a dissertation entitled: "The Effect of Mango Fibres on the Structural Properties of Concrete" in fulfillment of the requirements for the award of Master of Science in Structural Engineering degree of Kyambogo University.

Supervisor

Dr. Ssenyondo Vicent

Signature: …….

Date: …….

Supervisor

Dr. Kyakula Micheal

Signature: …….

Date: …….

ACKNOWLEDGEMENT

I hereby extend my sincere appreciation to the almighty God for having enabled pursue my education to this point. I also thank God for good relationship I have had with lecturers, fellow students, workmates and all those that I have rubbed shoulders with during this journey.

I acknowledge my supervisors Dr. Ssenyondo Vicent and Dr. Kyakula who worked tirelessly in supervising this research. I also extend my gratitude to Dr. Eng. Oleng Morris with whom I shared my research to offer me more guidance in the compilation of this proposal.

Finally, I would also like to thank my parents, siblings, relatives and friends for their financial and emotional support and encouragement they have offered me to complete this course.

To all those I may not have categorically acknowledged, but played a vital role during this period of training, may the Almighty God bless you all.

CONTENTS

LIST OF TABLES

LIST OF APPENDICES

LIST OF FIGURES

LIST OF ACRONYMS/ ABBREVIATIONS

ACI	American Concrete Institute
ASTM	American Standard for Testing of Materials
CML	Central Materials Laboratory
FEA	Finite Element Analysis
FRC	Fibre Reinforced Concrete
KyU	Kyambogo University
MFRC	Mango Fibre Reinforced Concrete
MPa	Mega Pascal
OPC	Ordinary Portland Cement
PC	Plain Concrete
PMM	Periodic Micromechanics
RVE	Representative Volume Element
SD	Standard Deviation
SEM	Scanning Electron Microscopy
UCS	Uniaxial Compressive Strength
UTM	Universal Testing Machine
UTS	Uniaxial Tensile Strength
W/C	Water to Content Ratio

LIST OF SYMBOLS

A_f	Cross-sectional area of mango fibres
e	Eccentricity
E	Young's modulus
ε	Strain
F	Average force
f_{cb}/f_c	Ratio of biaxial to uniaxial compressive strength at zero plastic strain
f_{ck}	Characteristic compressive cylinder strength of concrete at 28 days
f_{ctm}	Mean tensile strength of concrete
f_{cm}	Mean compressive strength of concrete
G	Shear modulus
K	Shape factor for the yield surface
ν	Poisson's ratio
σ	Stress

ABSTRACT

This study investigates the effect of mango fibres on the structural properties of concrete, focusing on mechanical performance, durability, and crack behaviour. Concrete's inherent brittleness limits its resistance to crack initiation and propagation, yet natural fibres have been identified as effective reinforcements. The study evaluated mango fibre properties, the performance of plain and mango fibre-reinforced concrete (MFRC), and the mechanical behaviour of MFRC using both experimental testing and finite element modelling.

A total of 351 C25 concrete samples were prepared, including 120 plain concrete specimens and 231 MFRC specimens with fibre contents of 0.1%, 0.25%, 1.0%, and 1.5% and fibre lengths of 30-, 40-, and 50-mm. Samples were tested at 7 and 28 days in accordance with ASTM, ACI, BS, and EN standards for fibre characterization, mixing, specimen preparation, curing, workability, mechanical testing, drying shrinkage, and water absorption. Experimental controls included use of calibrated equipment, standardized mixing and curing procedures, and consistent testing conditions to ensure reliability of results.

Results showed that mango fibres possessed a tensile strength of 616.96 MPa. Incorporation of fibres increased compressive, flexural, and split tensile strengths by 13.6%, 49.8%, and 16.8%, respectively, with optimal performance observed at 1.0% fibre content and 40 mm length. Mango fibres reduced drying shrinkage by up to 100%, thereby limiting crack development, although water absorption increased by up to 22.4% at higher fibre contents. ABAQUS simulations of a representative volume element further demonstrated improved crack resistance and delayed failure in MFRC compared to plain concrete.

This study addresses the limited research on the structural use of mango fibres in concrete, particularly regarding their influence on strength, shrinkage, and crack behaviour. The integrated experimental and numerical results provide mechanistic insight into fibre bridging and post-cracking stiffness. These findings demonstrate the practical potential of MFRC for improved crack control, enhanced structural resilience, and sustainable utilization of agricultural waste within Uganda's construction sector.

CHAPTER ONE: INTRODUCTION

1.1 Background

Concrete remains the most widely used construction material due to its versatility, durability, and economy. However, its production consumes vast quantities of non-renewable natural resources and energy, while generating significant carbon emissions (Tinni et al., 2013). The main raw materials for concrete production are cement, aggregates and water pose sustainability concerns as aggregates sourced from quarries are finite and environmentally taxing (Janamian and Aguiar, 2023). The reuse of industrial by-products and renewable resources, such as natural fibres, has emerged as an effective strategy to reduce reliance on non-renewable materials and enhance the sustainability of concrete (Hosseini et al, 2023).

For decades, fibres have been used as reinforcements in composites to enhance mechanical and durability properties (Habibi et al., 2023). When appropriately selected, fibres improve tensile and flexural strengths, control shrinkage cracking, and increase concrete's toughness and service life (Anas et al., 2022; Wafa, 2008).

Synthetic fibres such as polypropylene and glass remain common in practice due to their high tensile strength and ductility (Casamatta, 1986). However, their production is costly and environmentally unsustainable, with relatively high carbon footprints (Roesler et al, 2006). Consequently, attention has shifted toward natural fibres as affordable, renewable, and biodegradable alternatives with lower environmental impact (Kavitha et al, 2017).

Natural fibres, however, are hydrophilic and susceptible to moisture absorption, which weakens fibre–matrix bonding (Shadheer et al, 2021). To mitigate this, fibres are often subjected to surface modification or chemical treatment to improve interfacial adhesion and moisture resistance (Adekunle, 2015).

The mechanical performance of fibre-reinforced concrete is highly dependent on the fibres' type, geometry, and durability in alkaline environments (Isabai et al., 2023; Jansson, 2008). Despite these challenges, natural fibres remain attractive due to their renewability, light weight, low cost, and potential to improve concrete performance (Oliveira et al., 2019).

In Uganda, mango processing generates large volumes of fibrous fruit waste that are typically discarded or left to decompose e.g., Teju juice processing factory generates approximately 32 tonnes of mango waste daily (Nanjala, 2025; Emwamu, 2020). This agro-industrial by-product represents an untapped, renewable resource that can be repurposed into reinforcement fibres for sustainable concrete production using locally available materials.

Preliminary studies however indicate that mango fibres possess mechanical strength comparable to other natural fibres such as jute and sisal, but limited research has investigated their role in enhancing the structural and durability performance of concrete (Reis et al., 2024). This gap presents an opportunity to assess the suitability of mango fibres as a sustainable reinforcement material in concrete. Thus, this study aims to determine the effect of mango fibres on the structural properties of concrete.

1.2 Problem statement

Drying shrinkage is a significant durability challenge in concrete structures, primarily resulting from the gradual loss of moisture from hardened concrete. This moisture loss generates internal tensile stresses, leading to a reduction in volume and the formation of cracks. In conventional concrete, drying shrinkage strains typically range between 400 and 800 micro-strains, which can cause visible cracking, increase permeability, and accelerate deterioration (Markovski et al., 2012; Moore, 2005). These cracks allow the ingress of harmful agents such as water, chlorides, sulfates, and carbon dioxide, which accelerate the corrosion of steel reinforcement, reduce the structure's service life, and, in severe cases, cause premature failure.

Controlling drying shrinkage is essential to maintaining the mechanical integrity and long-term performance of concrete. Fibre reinforcement is a common solution, as fibres reduce crack formation and propagation while improving strength and durability (Habibi et al., 2023). However, synthetic fibres, such as polypropylene and glass fibres are costly and environmentally unsustainable, with carbon footprints of approximately 1.85 kg CO_2e/kg and 2.2–2.9 kg CO_2e/kg, respectively (Anas et al., 2022; Kavitha et al, 2017; Wafa, 2008 and; Casamatta, 1986).

Natural fibres such as jute, sisal, and banana have emerged as sustainable and affordable alternatives to synthetic fibres, attracting growing interest due to their environmental benefits. These fibres are biodegradable, renewable, and locally available, and have shown promise in minimizing drying shrinkage while enhancing the mechanical strength and

durability of concrete. (Marina et al., 2021; Kavitha et al, 2017). However, limited research has examined the structural performance of concrete reinforced with mango fibres, a readily available agricultural by-product with comparable tensile characteristics and strong interfacial bonding potential. The specific influence of mango fibres on drying shrinkage, crack control, and mechanical properties remains underexplored**,** creating a critical gap in understanding their structural effectiveness.

Addressing this gap is significant to structural engineering practice**,** as identifying a sustainable fibre alternative that mitigates shrinkage and improves structural performance could extend service life, reduce maintenance costs, and advance environmentally responsible construction.

1.3 Research objectives

1.3.1 Main objective

To investigate the performance of mango fibres in enhancing the structural properties of concrete.

1.3.1 Specific objectives

i. To characterize the physical and mechanical properties of mango fibres relevant to concrete performance.
ii. To determine effect of mango fibre length and fibre content on drying shrinkage, water absorption, compressive, tensile and flexural strength of concrete.

iii. To model the mechanical behaviour of Mango Fibre Reinforced Concrete using Finite Element Analysis.

1.4 Research questions

i. Do mango fibres possess physical and mechanical properties (e.g., tensile strength, elongation, diameter) within ranges suitable for structural reinforcement in concrete?

ii. What is the effect of mango fibre length and fibre content on drying shrinkage, water absorption, compressive, tensile and flexural strength of concrete?

iii. How accurately can Finite Element Analysis model the mechanical performance of Mango Fibre Reinforced Concrete?

1.5 Justification of the study

Natural fibres are renewable, biodegradable, and low-cost materials that enhance concrete performance by improving mechanical strength and resistance to cracking, contributing to material innovation in line with Sustainable Development Goal 9, Target 9.5 (Marina et al., 2021; Pandalai, 2018; UNGA, 2015). Despite their potential, fibrous mango waste from processing facilities such as the Teju juice factory is frequently discarded. This research promotes its reuse in concrete, aligning with Sustainable Development Goal 12, Targets 12.2, 12.3, and 12.5, by encouraging sustainable resource management, reducing food-related waste, and supporting recycling practices. Furthermore, integrating mango fibres into concrete as a value-added material supports productivity and innovation within the construction industry, contributing directly to Sustainable Development Goal 8, Target 8.2 (UN, 2015).

Figure 1.1 Mango waste at Teju juice factory

1.6 Significance

This study on the effect of mango fibres on the structural properties of concrete could offer the following valuable benefits to local communities, academia, regulatory bodies, waste management authorities, and construction professionals including:

i. Providing low and middle-income earners with an affordable and locally accessible material (i.e., mango fibres) to enhance concrete performance and promote sustainable, cost-effective construction solutions.

ii. Offering academia and regulatory agencies critical insights into natural fibre-reinforced composites, establishing a scientific foundation for future research and informing regulatory standards for the use of agro-waste in construction materials.

iii. Assisting waste management authorities by demonstrating the potential for reutilizing mango processing residues, thereby encouraging sustainable waste management practices aligned with circular economy principles.

iv. Equipping construction engineers with practical knowledge on the structural benefits of incorporating mango fibres into concrete, fostering the adoption of innovative and environmentally responsible materials within the construction industry.

1.7 Scope of the study

This section provides boundaries or limits within which this research was conducted.

Mango fibres were obtained from mango waste discarded at Teju juice factory while concrete ingredients were sourced within Kampala metropolitan area. Laboratory tests were conducted from Busitema University and Kyambogo University.

A total of 351 samples were prepared from C25 concrete mix design and comprised of 6 mixes of plain concrete (reference concrete) and 231 samples of mango fibre reinforced concrete of varying fibre content (at 0.1%, 0.25%, 1.0% and 1.5%) and length (30, 40 and 50) mm. The samples were tested at 7 and 28 days for compressive strength and at 28 days for; tensile strength, flexural strength, water absorption and drying shrinkage. Tensile, flexural and compressive strength were determined using the Universal Testing Machine (UTM). The behavioural performance of mango fibre reinforced concrete and plain concrete was modelled using ABAQUS FEM and the results compared.

Experimental testing for drying shrinkage, flexural strength, split tensile strength and water absorption was conducted after 28-days while Compressive strength was done at 7- and 28-days.

1.8 Conceptual framework

This research is guided by the conceptual framework that illustrates the relationship between inclusion of mango fibre into concrete to enhance the structural properties of concrete as shown in Figure 1.2. The independent variables are mango fibre length and content and concrete constituents and the dependent variable is the structural performance of concrete in tensile strength, flexural strength, compressive strength, drying shrinkage and water absorption. The intermediating (moderator) variables are mango fibre treatment and concrete mix design.

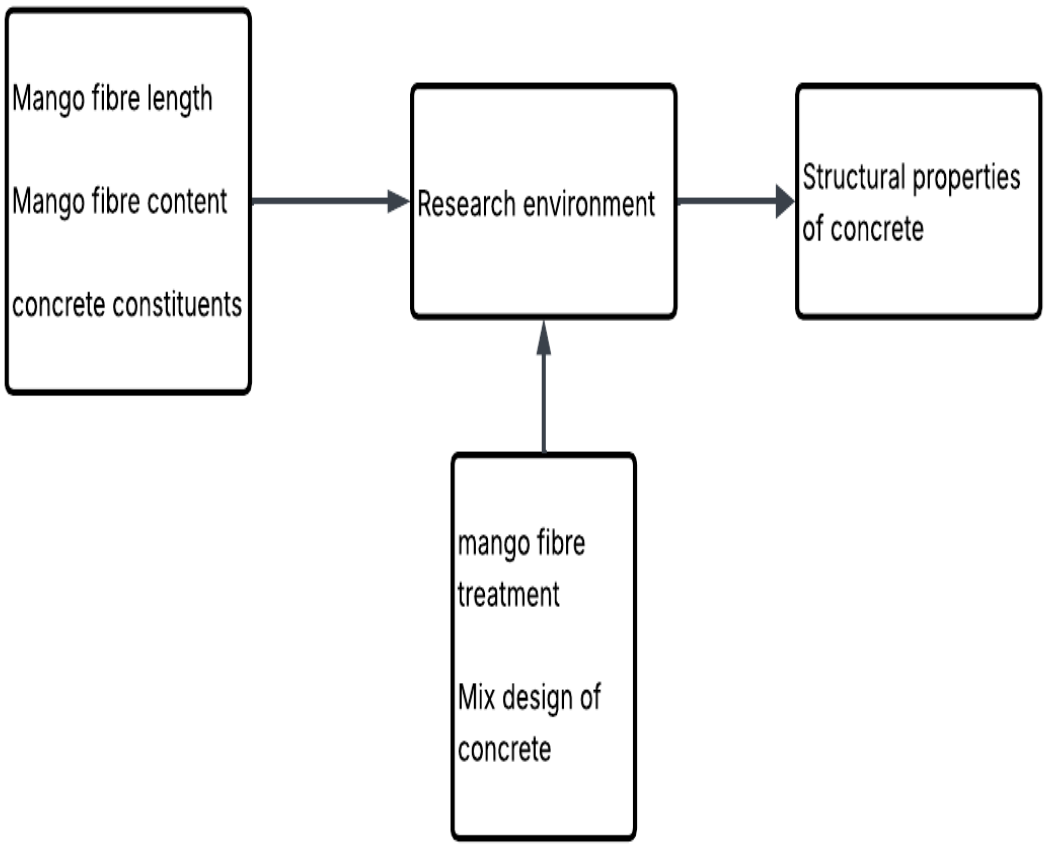

Figure 1.2 Conceptual framework

CHAPTER TWO: LITERATURE REVIEW

2.1 Introduction

This chapter reviews the literature relevant to the use of natural plant fibres, particularly mango fibres, as reinforcement in concrete. It covers fibre classification, chemical and physical composition, extraction and pre-treatment methods, mechanical properties, fibre–matrix interactions, comparative performance versus synthetic fibres, finite element modelling (as applied to fibre-reinforced concrete), commonly reported in the literature. Throughout the review, emphasis is placed on findings that directly inform the aims and objectives of this study: to evaluate how mango fibres affect the structural properties of concrete.

2.2 Natural fibre classification and processing effects on fibre properties

Natural fibres are gaining research and industrial interest as sustainable, low-density reinforcement alternatives to synthetic fibres (e.g., glass, carbon, aramid). They offer lower embodied energy and improved biodegradability, but typically show greater variability in properties and more sensitivity to environmental exposure (moisture, biological attack) (Habibi et al., 2023).

Use of agricultural residues (including mango by-products) may reduce waste streams while providing local, low-cost reinforcement resources for concrete applications. Several recent reviews highlight the trend toward valorization of mango waste and other African natural fibres in polymer and cementitious composites (Mohankumar et al, 2021).

2.2.1 Classification of natural fibres

Natural fibres are classified by origin: plant (cellulosic), animal (protein based), mineral and microorganism-derived. For concrete applications the focus is almost always on plant fibres (stem, leaf, seed/fruit residues) (Pramendra Kumar et al., 2018). Plant fibres commonly studied for cementitious composites include sisal, jute, coir, banana, bamboo and, increasingly, mango residues (peel, seed shell, and fibre bundles) (Karimah et Al., 2021). Plant fibres are attractive because of high specific strength and low density, but require treatment to address moisture affinity and compatibility with hydrophobic matrices (Habibi et al., 2023).

2.2.1.1 Chemical constituents of natural fibres

Fibres consist of both a primary and a secondary wall. The primary wall is made up of hemicellulose, pectins, proteins, and loosely arranged cellulose microfibrils, which contribute to its flexibility. (Habibi et al., 2023). The secondary wall is stiffer and is responsible for the fibres' mechanical properties.

The secondary wall contains the same constituents except richer in cellulose and contains lignin (Pramendra Kumar et al., 2018). Natural fibre composition is dependent on its botanical origin, climatic conditions, maturity and method of extraction (Habibi et al., 2023). Table 2.1 exhibits the chemical composition of natural fibres.

Table 2.1 Chemical composition of natural fibres

Fibre	**Cellulose (wt%)**	**Hemicellulose (wt%)**	**Lignin (wt%)**
Bamboo	22.8 – 56.7	17.2 – 43.8	21 - 31
Canary	7.2 – 41.7	19 – 22.9	-
Corn	41.7	46	7.4
Sugar cane bagasse	41.1 – 55.2	16.8 – 31.8	22.3 – 25.3
Sisal	60 -78	10 – 38.2	8 - 14
Cotton	82.7 - 92		0
Oil palm	47.91 - 65	19.06	24.45 - 29
Pineapple leaf	70 - 82	18	5 – 12.7
Rice husk	35 - 45	19 – 28	20
Banana	60 - 65	10 – 24	5 - 10
Hard wood	31 - 64	25 – 40	14 - 34

(Habibi et al., 2023)

It should be noted that the cellulose fraction supplies tensile stiffness while surface lignin/hemicellulose content explains expected hydrophilicity and the need for surface modification through fibre treatment.

2.2.1.2 Physical characteristics of natural fibres

Natural fibres present an environmentally friendly reinforcement option for both general uses and specialized components. Their recyclability and carbon neutrality make them highly advantageous, and their natural properties can enhance composite materials especially by improving vibration damping and reducing overall weight. The physical characteristics of different natural fibres are summarized in Table 2.2.

Table 2.2 Physical properties of natural fibres (Habibi et al., 2023)

Fibres	**Fibre length (mm)**	**Fibre diameter (mm)**	**Thickness of single cell wall (micron)**	**Width of lumen (micron)**
Cotton	15.0 – 56.0	10.0 – 45.0	3.6 - 3.8	15.7 – 16.4
Jute	0.8 – 9.0	5.0 – 30.0	5.2 – 11.3	3.4 – 7.6
Flax	10.0 – 65.0	5.0 – 38.0	10.0 – 20.0	2 - 40
Hemp	5 - 40	15 - 40	2 - 15	0.5 - 10
Ramie	30.0 – 60.4	25 - 30	9 - 16	12 - 82
Sisal	0.8 – 8.0	7.0 – 47.0	8.0 – 25.0	8.0 – 12.0
Coconut coir	0.3 – 1.0	12.0 – 14.0	0.06 – 8.0	13.59
Softwood craft	2.5 – 5.9	25 - 50	2 - 8	16.87 – 27.23
Sugar can bagasse	0.7 – 2.8	10.0 – 40.0	1.4 – 9.4	1.0 – 1.19
Pineapple leaves	3.0 – 9.0	5.9 – 80.0	1.8 – 8.3	2.4 - 3

Table 2.2 Continued

Banana	0.1 – 4.2	12.0 – 30.0	1.2 – 1.5	13.4 – 22.4
Areca	10 - 60	379 - 476	10 - 20	2 - 4
Oil palm	0.6 – 1.4	8.0 – 25.0	1.7 – 2.2	6.9 – 9.8
Rice husk	0.4 – 1.2	8.0 – 15.5	2.0 – 5.6	1.1 – 8.7
Bamboo	2.0 – 3.0	14.0 – 17.8	3.0 – 9.0	3.8 – 9.6
Corn husk	0.4 – 1.4	12.1 – 26.7	2.4 – 6.5	2.4 – 20.1

2.2.1.3 Mechanical properties of natural fibres

Natural fibres can undergo various processing methods to produce reinforcement materials with differing mechanical characteristics. The properties and internal structure of these fibres are affected by multiple factors, including the plant's growth stage, age, and the environmental conditions in which it develops (Adekunle, 2015).

The tensile strength of natural fibres is affected by the length of the specimen used during testing, as well as by the degree of fibre refinement (Shadheer et al, 2021). Table 2.3 provides some detail on mechanical properties of natural fibres

Table 2.3 Mechanical properties of natural fibres (Adekunle, 2015)

Fibre	**Density (g/ cm^3)**	**Tensile strength (MPa)**
Cotton	1.5 – 1.6	287 - 597
Jute	1.3	393 - 773
Flax	1.5	345 - 1035
Hemp	1.4 – 1.6	690

Table 2.3 Continued

Ramie	1.5	400 - 938
Sisal	1.5	511 - 635
Coconut Coir	1.2	175
Soft wood kraft	1.5	1000
Sugar can bagasse	1.2 – 1.42	290 - 6127
Pineapple leaves	0.8 – 1.60	413 - 1627
Banana	0.322 – 1.35	55 - 68
Areca	0.78 – 1.25	147 - 322
Oil palm	0.7 – 1.55	60 - 81
Rice husk	0.1 – 0.3	19 - 135
Bamboo	0.6 – 1.1	100 - 1000
Corn husk	1.18 – 1.49	332.57 – 345.16

2.2.2 Extraction methods for natural fibres

Extracting natural fibres from their source is a critical step that determines the quality, purity and mechanical performance of the resulting reinforcement material. For plant fibres, extraction typically involves separating the fibrous bundles from the plant matrix, removing lignin, pectin and other binding substances. Common extraction techniques include;

i. Mechanical (Decortication) method: It is method commonly used in extraction of natural fibres from plants with fibrous stems such as hemp, flax and jute. This method is done mechanically (manually) or chemically, depending on the plant and processing conditions. In this method, the outer part of the stem (i.e., the bark) is removed there by exposing the inner fibres (Rao and Rao, 2007).

ii. Blow molding method: This technique serves to isolate fibres from bamboo. It involves heating and softening the bamboo fibres with the aid of a screw header. Thereafter, the fibres are blown through a cooling chamber and the end product are continuous fibres which are of high quality and adequate mechanical strength (Habibi et al., 2023).

iii. Enzymatic method: With this method, natural fibres are extracted using specific enzymes. These enzymes break down the non-fibrous components of plants and the end-product are high quality fibres with low impurity content.

Extraction strongly influences the morphology, surface chemistry and mechanical behaviour of fibres. Inadequate extraction can leave residual pectin and lignin, leading to poor bonding in cementitious systems. Conversely, over-processing may shorten fibres and reduce tensile strength.

For mango residues, mechanical scraping followed by water retting and sun drying has been found effective for isolating fibres suitable for composite use (Ferreiro, 2024). The selected method for this study (alkaline–mechanical extraction) reflects a balance between

fibre purity, surface activation and strength retention, consistent with approaches reported for banana and sisal fibres in Uganda (Atima, 2022)

Consequently, the extraction approach adopted in this study, mechanical–alkaline treatment followed by air drying, was selected to produce fibres with sufficient cleanliness for good bonding while preserving their natural strength, consistent with the goal of evaluating mango fibres as reinforcement in concrete.

2.2.3 Pre-treatment of natural fibres and its impact.

Natural fibres are hydrophilic which leads to weak adhesion and moisture absorption which causes weak compatibility in bio-composites. Therefore, natural fibres must be pretreated in order to increase the biocompatibility between the fibres and matrix by the activation of the fibres' hydroxyl groups (Habibi et al., 2023). Fibres undergo physical or chemical treatments to enhance the adhesion between the fibre and the matrix (Adekunle, 2015); -

2.2.3.1 Chemical treatment

Cleaning the fibre surface chemically can change its composition, leading to lower moisture absorption, better resistance to wear, altered mechanical behaviour, and increased thermal stability (Habibi et al., 2023). The major constituent of the fibres that is the target for chemical modification is Cellulose. Chemical modification decreases the fibres' moisture uptake, strengthening the interface and yielding composites with better mechanical performance (Adekunle, 2015).

i. Enzymatic treatment of fibre

This method of treatment eliminates binders such as waxes and lignin found on surfaces of untreated fibres. However, fibrillation and damage to treated fibres has been observed (Hosseini et al, 2023).

ii. Acetylation treatment

Acetylation is frequently employed to alter the surface characteristics of plant-based fibres, enhancing their thermal resistance and decreasing their affinity for water. This surface modification occurs through a chemical interaction between the hydroxyl groups present in the fibres and acetyl groups (CH_3CO), resulting in a more hydrophobic outer layer (Pramendra Kumar et al., 2018).

Prior to the main reaction, fibres are often pre-soaked in acetic acid to optimize the process. Typically, the treatment duration spans between one and three hours. Beyond its effectiveness in reducing moisture absorption, this method has been reported to increase the fibres' thermal stability (Adekunle, 2015).

2.2.3.2 Physical treatment

Physical modification techniques, such as fibre stretching, calendaring, heat treatment, and yarn formation, do not alter the fibres' chemical composition. However, they do affect the structural configuration and surface characteristics, thereby impacting the quality of mechanical adhesion with polymer matrices (Adekunle, 2015).

Additional physical approaches include treatments like corona discharge and cold plasma application. Corona discharge, in particular, modifies the surface energy of cellulose fibres and is commonly used to initiate surface oxidation processes (Adekunle, 2015).

Another notable method is mercerization, which involves treating cellulose fibres with an alkaline solution to enhance their surface and structural properties (Habibi et al., 2023).

i. Alkaline treatment with caustic soda

Often referred to as mercerization, this chemical treatment involves immersing plant fibres in an aqueous sodium hydroxide (NaOH) solution. This exposure causes the fibres to undergo considerable swelling, along with changes in cellular structure, size, morphology, and mechanical behaviour (Hosseini et al, 2023).

The reaction of NaOH with cellulose can be represented as follows; -

$$C_6H_{10}O_5 - OH + NaOH \longrightarrow (C_6H_{10}O_5 - O) + Na^+ + H_2O \quad (2.1)$$

(Habibi et al., 2023)

Through this alkaline process, surface impurities such as lignin, hemicellulose, and pectin are removed from the fibre cell walls. This cleaning action improves surface activation, enhances tensile strength, and increases surface roughness factors that significantly contribute to improved physicochemical bonding at the fibre–polymer interface (Yimer and Gebre, 2023).

Moreover, alkaline treatment introduces alterations in the fibres' size, shape, and mechanical attributes. However, the NaOH concentration must be carefully controlled,

as higher levels can reduce fibre crystallinity; an important structural feature needed for optimal mechanical performance (Adekunle, 2015). Numerous studies further confirm that alkalization contributes to improved thermal resilience of the treated fibres (Habibi et al., 2023).

ii. Thermal drying

Thermal drying of natural fibres before composite fabrication is essential for achieving desirable material performance. Excess moisture within the fibres can hinder effective adhesion at the fibre–matrix interface, thereby weakening the bond strength. Furthermore, the presence of water during processing may cause vaporization, which can generate voids within the composite structure. These voids often act as defect zones, leading to compromised mechanical integrity (Pramendra Kumar et al., 2018).

2.3 Fibre-matrix bond mechanisms for natural fibre reinforced concrete

The performance of natural-fibre composites is governed largely by the efficiency of load transfer across the fibre–matrix interface. While most authors agree that hydrophilicity of plant fibres weakens this interface, studies differ on how significant this effect is and how best to mitigate it. For example Shadheer et al (2021) emphasizes the role of mechanical protection and stress transfer but did not address moisture-related incompatibility, whereas Hosseini et al (2023) explicitly attribute the poor interfacial bond to polarity mismatch between hydrophilic fibres and the hydrophobic cement matrix. Together, these findings suggest that surface chemistry, rather than just mechanical embedding, is a critical determinant of bond quality.

There is consistent evidence that natural fibres bond less effectively than synthetic fibres; however, researchers disagree on whether this is primarily due to surface roughness or to moisture sensitivity. Hosseini et al (2023) attributed the superior bonding of synthetic fibres to their smoother, inert surfaces, while other studies argue that the absence of swelling-related micro-voids is the dominant advantage. This variation highlights the need to investigate fibre swelling behaviour specifically for mango fibres.

Surface treatments provide another area where findings converge but explanations vary. Chemical modification is widely reported to improve fibre–matrix adhesion (Habibi et al., 2023; Adekunle, 2015). However, the mechanisms differ: one school attributes the improvement to the removal of waxes and surface impurities Adekunle (2015), whereas other attributes it primarily to reduced water absorption and lower risk of debonding under load (Habibi et al., 2023). Although both perspectives indicate that pre-treatment is beneficial, the differing interpretations show that the exact governing mechanism is not fully resolved.

Comparative studies consistently demonstrate that treated fibres outperform untreated ones, with flexural strength improvements commonly ranging from 10–25% (Habibi et al., 2023). However, variations in experimental procedures, fibre species, and treatment severity limit the generalizability of these results. This inconsistency reinforces the need to evaluate how mango fibres, whose chemical composition differs from more widely studied natural fibres, interact with the cementitious matrix.

2.3.1 Effect of fibre orientation

Fibre alignment within a composite matrix is a key factor that significantly affects the performance of fibre-reinforced materials. The directional arrangement of fibres strongly impacts properties such as tensile strength, stiffness, and toughness (Hosseini et al, 2023).

When fibres are aligned parallel to the direction of applied load, typically referred to as 0° orientation, they tend to exhibit superior tensile strength due to more efficient load transfer along their length, stiffness and toughness (crack propagation in the composite) than those oriented perpendicular to the load direction (Habibi et al., 2023).

2.3.2 Comparison between natural fibre and synthetic fibre composite properties

Natural and synthetic fibres have both been used as reinforcement materials in concrete and polymer composites. Synthetic fibres such as glass, carbon and polypropylene generally exhibit higher tensile strength, stiffness and durability compared to natural fibres. However, they are costly, energy-intensive to produce and non-biodegradable, which limits their sustainability in developing contexts (Hosseini et al, 2023).

When comparing the mechanical performance of fibre-reinforced composites, those incorporating synthetic fibres, particularly carbon fibres, typically demonstrate superior strength and stiffness relative to their natural fibre counterparts. Despite this, natural fibre composites are often favored for their lower density, which contributes to a reduced specific weight (Habibi et al., 2023).

In terms of durability, synthetic fibre composites usually exhibit enhanced resistance to environmental degradation, including moisture, microbial attack, and chemical exposure. Conversely, natural fibre composites are more prone to such degradation and often require surface treatments or additives to enhance long-term performance (Habibi et al., 2023).

Regarding environmental sustainability, natural fibre composites offer a distinct advantage. Their renewable nature and higher biodegradability make them a more eco-conscious alternative to synthetic fibre composites, which tend to be derived from non-renewable sources and degrade more slowly (Hosseini et al, 2023).

2.4 Finite element modelling of fibre reinforced concrete

Finite Element Analysis is a numerical method commonly used in engineering and the physical sciences to simulate how complex systems and structures respond to different conditions. It is essentially a numerical approach utilized to predict the solutions of boundary value problems (Rao, 2004).

The method works by breaking down a complex geometry into a mesh of smaller, discrete units known as finite elements. These elements, such as triangles or quadrilaterals in two-dimensional models, or tetrahedral and hexahedral elements in three dimension, are governed by mathematical models that simulate their response to applied forces, environmental loads, and boundary constraints (Barbero, 2013).

A wide range of commercial software packages with FEA capabilities are available for solving engineering problems across different fields. These tools can handle both simple and highly complex analyses, ranging from linear elastic behaviour to fully nonlinear,

time-dependent simulations. Specialized software such as ABAQUS and ANSYS includes advanced modules for modeling composite materials, as well as allowing for user-defined material models and custom finite elements (Barbero, 2013).

Typically, modern FEA platforms are divided into three main stages: pre-processing, solution (processing), and post-processing. During the pre-processing phase, the user defines the geometry, assigns material properties, and selects appropriate element types. Loads and boundary conditions are specified at this stage or during the solution phase. The processing stage involves generating the global stiffness matrix and force vector, which are used to solve the system of algebraic equations; resulting in nodal displacements. Finally, in the post-processing stage, output data such as stress, strain, and failure metrics are computed and visualized. Most commercial post-processors offer graphical tools such as contour plots and deformation visualizations for detailed analysis (Lawrence et Al., 2019; Barbero, 2013).

Finite Element Analysis provides a computational approach to predict structural behaviour under loading. In studies of fibre-reinforced concrete, FEA has been applied to assess stress distribution, crack propagation, and fibre–matrix interaction (Ali et al., 2022). For this research, FEA offers a framework for modelling the influence of mango fibres on the mechanical response of concrete, complementing experimental observations.

2.4.1 Failure theories used in finite element analysis

Failure criteria are essential for predicting the onset of cracking, yielding, or structural collapse in concrete and composite materials. In the context of MFRC, failure theories

help assess how fibres influence stress redistribution and crack development under mechanical loading. The present study used two main criteria: Von Mises stress and Maximum Principal Stress, each offering insight into different failure mechanisms

i. Von Misses stress criterion: The Von Mises criterion is extensively used for ductile materials and evaluates failure based on the distortion energy in the material. It reduces the complex multiaxial stress state into an equivalent stress, allowing comparison with the material's yield strength (Anderson, 2006). In concrete modelling, Von Mises stress is useful for identifying regions where shear-dominated failure or yielding is likely to occur (Desai, 2012). Although concrete is semi-ductile, this criterion provides valuable insight into the initiation of inelastic behaviour, especially in natural fibre-reinforced composites where ductility increases due to fibre bridging.

ii. Maximum principal stress criterion: This criterion assesses the largest principal stress within a structure, anticipating failure when it exceeds the material's ultimate tensile or compressive strength (Desai, 2012). This criterion is particularly appropriate for brittle materials such as plain concrete, which fail predominantly in tension. In FEA of MFRC, it helps identify tensile cracking zones and evaluates how fibres affect crack initiation and propagation. The reduction in maximum principal stress in MFRC relative to plain concrete indicates the beneficial stress-sharing mechanisms introduced by the fibres.

2.4.1.1 Relevance to the study

i. The Maximum Principal Stress criterion is suitable for modelling the tensile failure of concrete, which is governed by crack initiation and propagation. This aligns with the simulation of the MFRC tensile test.

ii. The Von Mises criterion supports analysis of compressive behaviour by identifying regions where yielding or inelastic deformation develops under uniaxial compression. This corresponds directly to the compressive loading conditions modelled in this study.

2.4.2 Finite element approaches for fibre reinforced concrete

Finite Element Analysis has been widely applied in the study of fibre-reinforced concrete to understand mechanical behaviour beyond what can be observed experimentally. Two main modelling approaches are commonly used in the literature: macro-modelling**,** where concrete is treated as a homogeneous composite with averaged properties, and micro-modelling**,** where fibres and matrix are represented explicitly (Barbero, 2013; Mobasher, 2012). Micro-modelling provides greater insight into fibre–matrix interaction, crack initiation, and stress redistribution, but is computationally intensive.

A practical compromise is the Representative Volume Element (RVE) approach, where a small but statistically representative sample of the composite is simulated with explicit fibre geometry. This method has been used to investigate fibre pull-out, load transfer mechanisms, and enhancement in tensile and compressive behaviour of natural fibre composites (Barbero, 2013).

Given the heterogeneous nature of mango fibre-reinforced concrete, the RVE approach offers a suitable balance between computational efficiency and mechanistic accuracy for the present study.

2.4.3 Representative Volume Elements (RVEs) in composite modelling

An RVE is defined as the smallest volume over which material properties can be considered statistically homogeneous (Ferretti et Al., 2021). In concrete composites, RVEs are used to simulate the behaviour of inclusions such as fibres, voids, or aggregates, allowing researchers to study how local microstructural features affect global mechanical response. For fibre-reinforced concrete, RVE modelling captures fibre orientation, spacing, and volume fraction, making it a useful tool for understanding stress concentration and crack initiation patterns (Mobasher, 2012).

RVE models are particularly effective when experimental determination of micro-scale behaviour is difficult or destructive. By modelling fibre distribution and interaction with the cement matrix, RVEs can approximate stiffness changes, tensile crack development, and compressive load redistribution. This makes the method well suited for materials like mango fibre-reinforced concrete, where the performance depends heavily on micro-scale fibre behaviour.

2.4.4 FEM application in compressive and tensile response of concrete

Finite Element Analysis has been widely used to simulate the tensile and compressive response of concrete, providing insight into stress development and failure initiation under

uniaxial loading. Several studies have shown that FEA can effectively reproduce the brittle tensile cracking behaviour of plain concrete and the gradual stiffness reduction associated with fibre reinforcement (Zhang et al., 2018; Mobasher, 2012). Under compression, FE models have been used to evaluate crushing patterns, strain localization, and the influence of inclusions on load redistribution (Elbehiry et al., 2020).

In fibre-reinforced concrete, simulation enables examination of how fibres modify the failure mode by bridging developing cracks, reducing peak tensile stresses, and promoting more uniform stress distribution. These numerical insights complement laboratory testing by revealing internal stress mechanisms that are difficult to observe experimentally. For this study, FEM is particularly relevant for comparing how plain concrete and MFRC respond to tensile and compressive loads, thereby helping to interpret the experimentally observed improvements in failure resistance.

2.5 Literature summary and research gap

The literature shows that natural plant fibres such as sisal, jute, banana and pineapple have been successfully incorporated into cementitious composites to improve tensile behaviour, crack resistance and ductility. Key factors influencing fibre performance include chemical composition, extraction method, treatment process, fibre geometry and dosage, all of which significantly affect fibre–matrix bonding and composite strength. Studies from tropical regions, including Uganda, have demonstrated the viability of several agricultural fibres in concrete, although performance varies widely due to differences in fibre structure and processing conditions. Research on composite modelling further shows that approaches such as macro-modelling, micro-modelling and representative volume

elements can be used to simulate fibre–matrix interaction, while finite element methods have proven effective in predicting stress distribution and failure mechanisms in fibre-reinforced concrete systems.

Although natural fibres such as sisal, jute, banana and pineapple have been widely studied as reinforcement in cementitious composites, there is almost no published research on mango (Mangifera indica) fibres used in concrete, either globally or within Uganda. Most existing work on mango fibres relates to polymer composites or bio-based boards, leaving a clear gap in understanding their behaviour in cement matrices. This is notable given the abundance of mango waste in Uganda and its potential as an inexpensive, sustainable reinforcement material.

Existing studies further show that fibre performance depends strongly on extraction method, chemical composition, treatment and dosage, but there is no comparative evidence showing how mango fibres perform relative to other tropical fibres commonly found in East Africa. Similarly, while regional studies have evaluated banana and pineapple fibre concretes, no research has characterized mango fibres grown under Ugandan conditions, even though environmental factors significantly influence fibre properties.

Finally, although Finite Element Analysis (FEA) has been applied to natural and synthetic fibre reinforced concrete, validated numerical models for natural fibre composites remain scarce, and no FEA model currently exists for mango fibre reinforced concrete. This limits the ability to predict mechanical behaviour and optimize mix design for structural applications.

CHAPTER THREE: METHODOLOGY

3.1 Introduction

This chapter outlines the data collection techniques and research design employed to carry out this study. This section provides a comprehensive overview of the procedures followed in this study, along with the approaches used to address the research questions stemming from the problem statement. The experimental study considered the following independent variables: (1) Plain concrete, (2) Mango Fibre Reinforced Concrete, (3) Fibre content, and (4) Fibre length. The effects of these variables on compressive strength, tensile strength, drying shrinkage, water absorption, and flexural strength were evaluated through experimental testing.

3.1.1 Research design and approach

The research design represents the conceptual structure of methods and techniques employed to meet the study's specific objectives (Megel and Heermann, 1993). This study adopted an experimental approach, focusing on how the independent variables: fibre content and fibre length, affect the dependent variables; namely the structural properties of concrete.

3.1.2 Research approach

The following approach illustrated below was used to address the research design.

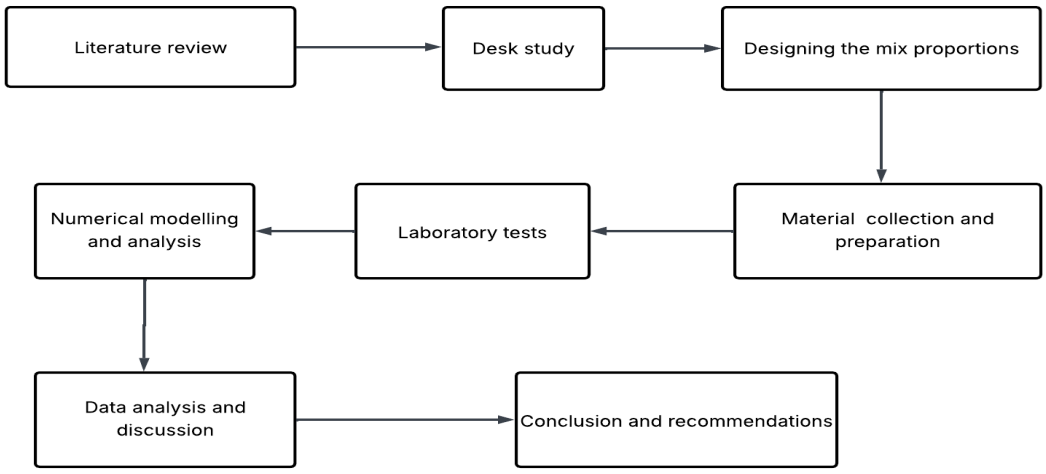

Figure 3.1 Research design and approach

A structured experimental program was developed to examine the impact of mango fibres on the structural properties of concrete, including tensile strength, flexural strength, compressive strength, drying shrinkage, and water absorption. Concrete mixes were prepared for both plain concrete (PC) and Mango Fibre Reinforced Concrete (MFRC). Table 3.1 summarizes the tested parameters along with their corresponding sample sizes, concrete types, and material quantities.

Table 3.1 Parameters to be tested at 7 and 28 days

Parameter	**PC**	**MFRC**	**Dimension (mm)**	**7 days**	**28 days**
Compressive strength	6 cubes	72 cubes	150*150*150	✓	✓
Flexural strength	3 beams	36 beams	750*150*150		✓

Table 3.1 Continued

Split tensile strength	3 cylinders	36 cylinders	100Φ*200	✓
Drying shrinkage	3 prisms	36 prisms	400*100*100	✓
Water absorption	3 cubes	36 cubes	150*150*150	✓

Compressive strength was measured at 7 and 28 days to capture early and standard-age strength development, while flexural strength, split tensile strength, drying shrinkage, and water absorption were measured only at 28 days**,** when the concrete has matured enough for reliable long-term performance assessment.

Table 3.2 Variables for the experiment are fibre length and fibre content

Fibre length (mm)	30mm	40mm	50mm
Fibre content	0.1%	0.1%	0.1%
	0.25%	0.25%	0.25%
	1.0%	1.0%	1.0%
	1.5%	1.5%	1.5%

As shown in Table 3.2, the fibre length was varied from 30mm, 40mm and 50mm for each fibre. The fibre content was varied from 0.1, 0.25%, 1.0% and 1.5%. Additionally, plain concrete served as the reference when investigating the effectiveness of incorporating mango fibres into concrete to improve the structural properties of concrete.

Table 3.3, 3.4 and 3.5 portray the number of samples that were prepared to determine the test parameters for this research.

Table 3.3 Samples cast for crushing compressive strength test for MFRC

Concrete age (days)	7 days			28 days		
Fibre content (%)	**Fibre lengths (mm)**			**Fibre lengths (mm)**		
	30mm	40mm	50mm	30mm	40mm	50mm
0.1%	3	3	3	3	3	3
0.25%	3	3	3	3	3	3
1.0%	3	3	3	3	3	3
1.5%	3	3	3	3	3	3

Table 3.4 Samples cast for crushing compressive strength test for plain concrete

Concrete age (days)	7 days	28 days
Fibre content (%)	**Fibre lengths (mm)**	**Fibre lengths (mm)**
	0	0
0.0%	3	3

Table 3.5 MFRC samples for drying shrinkage, water absorption, flexural and split strength tests

Fibre content (%)	**Fibre lengths (mm)**		
	30mm	40mm	50mm
0.1%	3	3	3
0.25%	3	3	3
1.0%	3	3	3
1.5%	3	3	3

A total of three plain concrete specimens were cast and used to evaluate drying shrinkage, water absorption, split tensile strength, and flexural strength, all assessed at 28 days.

Similarly, the samples for plain and mango fibre reinforced concrete were prepared in triplets in accordance with Clause 7.1 of BS EN 12390 which recommends a minimum of 3 samples so as to ensure integrity and reliability of experimental results.

The mean and standard deviation of each property were calculated to quantify variability. Error margins were determined as ± one standard deviation from the mean, and all results were reported accordingly. Observed deviations were analyzed to assess the reproducibility of the tests and the influence of fibre content and length on material performance.

3.1.3 Ethical considerations

All experimental work was conducted in accordance with standard laboratory safety protocols to ensure the safe handling and disposal of materials. Data were accurately recorded and reported, and all sources were properly acknowledged to uphold academic integrity.

3.1.4 Sample coding

To facilitate identification throughout the research process, each sample was assigned a unique code that reflected its concrete type, fibre length, fibre content and, concrete age. For example; M517 - D where; M – Mango fibres; 5 – fibre length (cm); 1 – Fibre content in ascending order; 7 – age of concrete at 7 days; - D – Casting date (i.e., dd/mm/yr)

3.1.5 Data collection

The materials used were; mango fibres, sand, aggregates, cement and water.

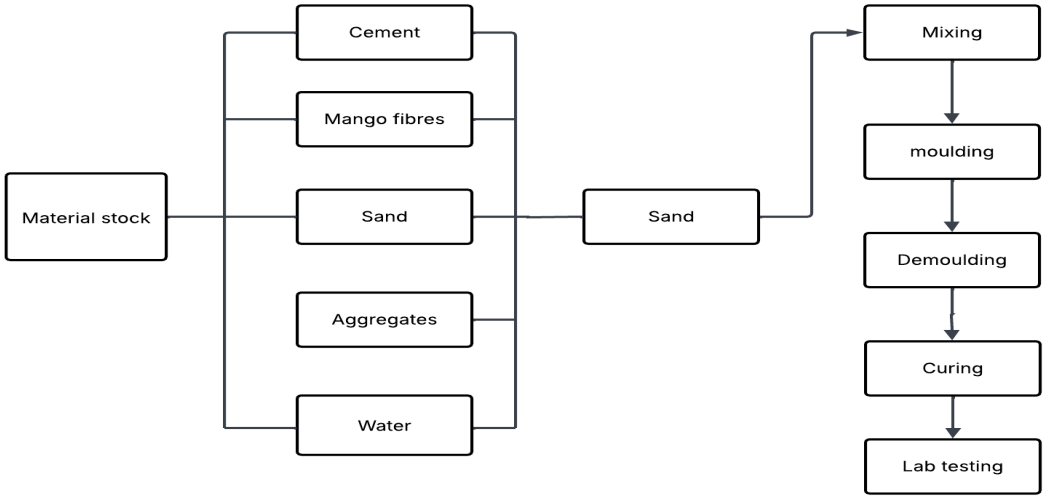

Figure 3.1 Material and sample preparation

3.1.4.1 Mango fibres

a) Identification of the source of mango fibres

Mango fibres were obtained from mango waste discarded at Teju juice factory in Soroti district. The factory generates approximately 32 tonnes of mango waste daily and processes fibrous Kagogwa mangoes for juice production

Figure 3.2 Air-drying washed mango fibres

b) Extraction of mango fibres

The procedure of extraction of mango fibres was based on one of the extraction techniques for natural fibres presented in (Rao and Rao, 2007). Manual extraction was the method used for mango fibre extraction and the following steps were followed;

i. The mangoes were thoroughly washed with water to remove juice that would cause fibres to stick to each other

ii. The mango fibre bundles were then combed and straightened with the aid of tooth picks to remove any entanglement and then left to dry in open air.

(a) Juice removal

(b) Combing mango fibres

Figure 3.3 Preparing mango fibres

c) Treatment process of mango fibres

The mango fibres were treated using Caustic Soda (NaOH) obtained from Sky Chem (U) LTD.

100g of Caustic Soda was dissolved in 5 liters (L) of distilled water to form a solution of 2% Sodium Hydroxide in at a liquor ratio of 50:1. Preparation of the solution is based on different research studies by (Yimer and Gebre, 2023) presented in section 2.6 of this research.

The raw mango fibres were then placed in the solution for 24 hours at temperature of 50°C since research according to (Yimer and Gebre, 2023; Hosseini et al, 2023) exhibited that optimal results for mechanical properties of natural fibres were achieved when natural fibres were subjected to mercerization for a period not longer than 48 hours and a temperature not greater than 50°C.

The treated or processed mango fibres were subsequently washed with a 1% (w/w) acetic acid solution to neutralize any residual sodium hydroxide (NaOH) on the fibre surfaces. This was to prevent alkali-silica reaction which would occur as a result of the high alkali content within the fibres reacting with silica present in aggregates to form an expansive gel that would cause the MFRC to expand, crack and deteriorate upon ingress of corrosive salts (Yimer and Gebre, 2023).

Finally, the mango fibres were washed with tap water.

(c) Chemical treatment of fibres

(d) Air-drying mango fibres

Figure 3.4 Processing mango fibres

3.1.4.2 Cement

ACI 544.1R-96 (2002), recommends Type I Ordinary Portland Cement for Fibre Reinforced Concrete (FRC). The cement complies with ASTM C150/ C150M – 20, 2020). Type III (high early strength) cement can be applied to reduce hardening delays caused by

glucose found in many natural fibres (Daniel et Al., 2002). For this research, CEM I 42.5N – OPC, manufactured by Tororo cement was used.

3.1.4.3 Water

Ordinary water fit for consumption was used for this research.

3.1.4.4 Aggregates

Crushed aggregates were obtained from Mbalala Quarry. The geological classification of the rock was determined from Kyambogo University - Concrete Laboratory. The maximum nominal size of crushed aggregates used for this research was 20mm.

3.2 Determination of physical and mechanical properties of mango fibres

Fibre properties were determined in accordance with ASTM Standards (ASTM C116/ C116M – 10a, 2015; ASTM D7357, 2019). Parameters to be investigated include; - tensile strength, breaking force, linear density, average diameter, stiffness and elongation break.

The single fibre tensile test was performed using a Universal Instron Testing Machine. The breaking load and elongation at failure were recorded at the point when failure occurs. The tensile strength of a single fibre was calculated using equation 3.1;

$$f_t = \frac{F}{A_f} \tag{3.1}$$

Where; f_t – tensile strength of a single fibre, A_f - cross-sectional area of the fibre

The average diameter of the mango fibres was measured using Scanning Electron Microscopy (SEM). The equipment used for assessing the geometric, physical, and mechanical properties of the fibres is summarized in Table 3.6.

Table 3.6 Mango fibre parameters and equipment requirement

Fibre parameter	**Equipment/Requirement**
Stiffness (mm)	FY2027B Stiffness tester
Weight (mg)	Precision balance
Fibre length (mm)	Steel half meter ruler
Linear density (g/cm^3)	Weight and length
Diameter (μm)	Tescan Vega 3 SEM
Breaking force (cN)	YG003E Single fibre tester
Breaking elongation (%)	YG003E Single fibre tester
Tensile strength (MPa)	Breaking force and diameter

3.3 Determination of the effect of mango fibre content and length on drying shrinkage, water absorption and mechanical properties of concrete

In order to evaluate the effect of mango fibre content and length on drying shrinkage, water absorption, compressive, tensile and flexural strength of concrete, concrete materials had to be tested and a mix design for plain (reference) concrete and mango fibre reinforced concrete prepared and these were discussed in the sub-sections that follow:

3.3.1 Tests on cement

Chemical and physical test certificates were provided by Tororo cement limited (Manufacturer) on purchase of cement and are presented in Chapter 4 of this research.

3.3.2 Tests on fine and coarse aggregates

The physical properties examined for coarse and fine aggregates included: aggregate type, sieve analysis, unit weight, specific gravity, moisture content, absorption, and gradation. The findings from these tests are presented in Chapter 4 of this report;

3.3.3 Mix design preparation

The mix design was developed based on the principle that concrete should ensure both adequate strength and prolonged durability of the structure. The selection of the desired properties was based on; anticipated exposure conditions, the type of structure and aggregate characteristics as explained in the subsequent sections. The nominal mix design that was selected for both plain and mango fibre reinforced concrete was C25.

a) Plain concrete

The standard used for plain concrete was based on the Department of Environment (DOE) method specified in BS 5328. Table 3.7 presents calculated mix design quantities for the plain concrete used in the experimental program. A detailed step-by-step procedure is provided in Appendix A.1.

Table 3.7 Mix design composition for plain concrete

Grade	Aggregates (mm)	Design slump (mm)	W/C	Materials Quantity (kg/m^3)			
				Cement (kg)	Water (kg or L)	Coarse aggregates (kg)	Fine aggregates (kg)
C25	20	30 - 60	0.5	64.0	32.0	97.0	206.1

b) Mango fibre reinforced concrete

The mix design for mango fibre reinforced concrete was prepared in accordance with the provisions given in ACI 544.1R-96 (2002). The quantities of mango fibres required in concrete was calculated relative to the amount of cement and the calculated quantities were provided in Table 3.8. To obtain quantities of fibres required for every individual batch, the following formulae were used;

Volume of concrete for each individual batch were computed using equation 3.2:

$$\left(\mathrm{V}_f \times \delta_f \times \mathrm{VFRC}\right) \times 1000g \tag{3.2}$$

Where; $\mathrm{V_{f-}}$ Fibre content (%), δ_f – density of treated mango fibres, $\mathrm{V_{FRC}}$ - Volume of FRC corresponding to each individual batch of individual length of fibres

$\mathrm{V_{FRC}}$ was obtained as follows,

$$\mathrm{V}_{FRC} = \frac{W_c}{c_c} \tag{3.3}$$

While densities of treated mango fibres, δ_f were obtained as follows;

$$\delta_f = \frac{M_f}{V_f} \quad (3.4)$$

Where; M_f - Mass of Treated mango fibres and V_f – Volume of mango fibres

Table 3.8 Calculated quantities of mango fibres used in the experiment

Fibre content (%)	Density of fibres (kg/m^3)	Mass (g)
0.1%	0.0221 kg/m^3	1.45 g
0.25%	0.0553 kg/m^3	3.64 g
1.0%	0.2212 kg/m^3	14.55 g
1.5%	0.3318 kg/m^3	21.83 g
Total		41.47 g

Table 3.9 provides the calculated mix design composition for Mango Fibre Reinforced concrete used for this experimental program. An in-depth sequential procedure is provided in Appendix A.2.

Table 3.9 Mix design composition for Mango Fibre Reinforced Concrete

Grade	Aggregates (mm)	Design slump (mm)	W/C	Mix proportions			
				Cement (kg)	Water (kg or L)	Coarse aggregates (kg)	Fine aggregates (kg)
C25	20	30 - 60	0.5	737.8	393.9	1194.1	2537.4

3.3.4 Mixing protocol

An electronically operated mechanical mixer equipped with rotating paddles was used for preparing the concrete mixes. The mixing procedure for plain concrete followed the guidelines outlined in BS 5328, while the mixing of Mango Fibre Reinforced Concrete (MFRC) adhered to recommendations in ACI 544.1R-96 (2002), which outlines two methods: (1) *wet mixing*, typically used for hand mixing, and (2) *dry-compacted mixing*. In this study, the *wet mixing method* was employed for both plain and fibre-reinforced concrete to ensure uniform dispersion of fibres and consistency in mix quality.

3.4.4.1 Precautions to be undertaken during mixing operation

During the mixing of mango fibre reinforced concrete, the following precautions were taken:

i. Mixing sequence: The materials were added in the order of aggregate: sand: cement: fibres: water. This sequence was adopted to minimize balling effect; which is the tendency of fibres to clump together during mixing.
ii. Fibre dispersion: Fibres were manually dispersed in small quantities during mixing until they were fully integrated into the mix.
iii. Mixing time: Mixing time for MFRC was increased by 120 seconds to ensure for a homogeneous mix.

Figure 3.5 Batching and fibre incorporation

3.3.5 Workability tests

For purposes of quality assurance, tests on freshly mixed concrete were conducted and these included; - slump tests, ambient temperature and concrete temperature measurements and these procedures were conducted in accordance with ASTM C143/C143M-20 (2020) Then moulds were smeared with oil using a scoop and concrete cast in the moulds was compacted in layers. Finally, finishing of the top face of the cast samples in the moulds was done concurrently with vibration to prevent fibres from protruding through the finished surface.

Figure 3.6 Slump test after concrete mixing

3.3.6 Curing

The concrete specimens were demoulded after 24 hours and then immersed in a curing tank for continued strength development. Curing was done in accordance with ASTM C31/ C31M-19, 2019.

3.3.7 Laboratory testing

Before carrying out any laboratory tests, all equipment used was checked to ensure it has the latest calibration certificates and that all systems were in good working conditions (i.e., The bearing surfaces were thoroughly cleaned of any foreign material). PPE such as safety overalls, safety boots, etc., were worn to ensure safety during sample preparation and testing.

Different standards were used to determine the different parameters for this research and these were summarized in Table 3.10.

Table 3.10 Summary of parameters to be tested

Test parameter	**Standard**
Compressive strength	BS 1881-116:1983
Split Tensile strength	BS 1881-116:1983
Drying shrinkage test	EN 12617- 4 -2002
Flexural strength	BS 1881-116:1983
Water absorption test	BS 1881-122:1983

3.3.7.1 Compressive strength test

This test was conducted in accordance with the standard testing procedures prescribed in BS 1881-116:1983 as follows:

Curing was carried out by immersing the concrete moulds/ cubes into a water bath until the date of testing. A Universal Testing Machine (UTM) with a maximum capacity of 3000 kN was used to conduct the compressive strength tests. Standard concrete cubes measuring 150 × 150 × 150 mm, in accordance with BS 1881-116:1983, were tested at both 7 and 28 days. Prior to testing, each cube was weighed, properly aligned, and centered on the UTM's loading platform. The load was then applied gradually until failure occurred, and the maximum compressive strength was recorded. The maximum compressive load was displayed on the screen of the UTM and was noted. The maximum axial load under compression measured was verified using equation 3.5;

$$F_c = \frac{P}{A} \tag{3.5}$$

Where; P – maximum crushing load (kN), A – area of concrete cubes (mm^2) and, F_c – Compressive cube strength (kN/mm^2) (Linhua Huang et al., 2024).

(e) Placing concrete mould on UTM's loading platform

(f) Reading compressive load from UTM screen

Figure 3.7 Compressive strength test

3.3.7.2 Split tensile strength test

This test was conducted in accordance with BS 1881-116:1983. The very Universal Testing Machine (UTM) used for the compressive strength test was employed to perform the split tensile strength test. Concrete cylinders were cured by immersion immersed in water for 28 days. After curing, the samples were extracted, surface-dried using a clean cloth, and then their dimensions were measured. The weight of each cylinder was recorded prior to testing.

The cylinders were then aligned and centred on the plate holder of the UTM. The recorded dimensions for the cylinders and weights were then uploaded into the machine and the machine was run. The machine exerted a load onto the sample until the specimen fractured. The maximum load is then displayed on the screen and recorded (Rasoul et al, 2023).

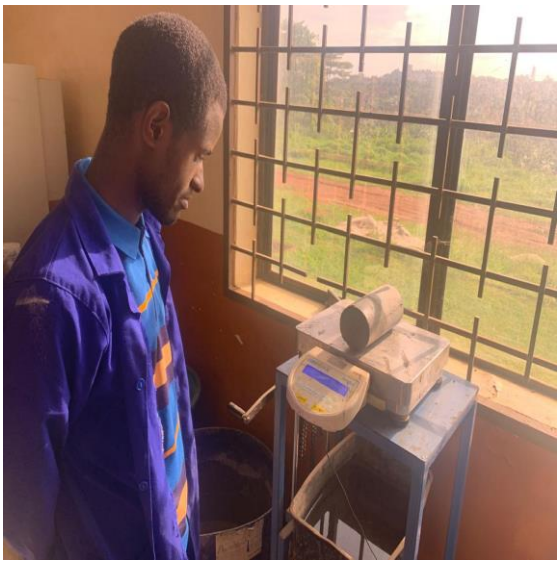

(g) Weighing concrete cylinder

(h) Exerting laod onto concrete cylinder

Figure 3.8 Split tensile strength test

3.3.7.3 Drying shrinkage test

The drying shrinkage test for both plain concrete and Mango Fibre Reinforced Concrete (MFRC) was conducted the standard procedures outlined in EN 12617-4-2002 (BS EN 12617-4, 2002). The dimension for length of freshly cast concrete in the prisms was measured (initial length). Curing was then carried out by immersing the concrete prisms into a water bath for 28 days. The prisms were removed from the water bath, surface-dried with a cloth, and their new lengths were measured. The change in length was then recorded to assess drying shrinkage.

Figure 3.9 Measuring concrete prism length

3.3.7.4 Flexural strength test

The flexural strength test was conducted following the procedures outlined in BS 1881-116:1983. To determine the flexural strength of MFRC, beam samples of 150 * 150 * 750 mm were tested under two-point loading. The same Universal Testing Machine (UTM) used for compressive and split tensile strength tests was employed to measure the peak load at failure of the specimens. The peak load was calculated using Equation 3.6:

$$f = \frac{3PL}{2bd^2} \tag{3.6}$$

Where; f – Flexural strength (N/mm^2), P – Peak load (N), L – span (350 mm) b- width (mm) and d (mm)

(i) Weighing concrete beam

(j) 2-point loading on concrete beam

Figure 3.10 Split tensile strength test

3.3.7.5 Water absorption test

The purpose of this test was to determine the rate of water absorption in both plain and Mango Fibre Reinforced Concrete (MFRC) by measuring the increase in specimen mass due to water uptake over time. The procedure followed the guidelines of BS 1881-122:1983 and aimed to assess the durability of the Mango Fibre Reinforced Concrete.

Concrete cubes were initially dried in a ventilated oven for at least 24 hours to obtain the dry mass, M_d. After drying, the specimens were fully immersed in a water bath for 24 hours. Following immersion, the samples were removed, surface-dried with a cloth, and weighed immediately to obtain the saturated surface-dry mass, M_w: The percentage of water absorption was calculated using the formula;

$$W_a(\%) = \frac{M_w - M_d}{M_w} \times 100 \tag{3.7}$$

Where; W_a – water absorption

; M_w = mass of saturated surface-dry specimen (wet mass)

; M_d = mass of oven-dried specimen (dry mass)

Figure 3.11 Oven-drying concrete cubes

3.4 Finite Element Modelling of the behavioural performance of MFRC and plain concrete

3.4.1 3D Representative Volume Element (RVE) model

The concept of the homogenization technique using a 3D Representative Volume Element (RVE) was employed in the Finite Element Analysis (FEA) to model the mechanical behaviour of mango fibres embedded in concrete. This approach allows for the estimation of effective macroscopic properties by accounting for the heterogeneous nature of the composite at the microscale. The modelling was carried out using SIMULIA ABAQUS Version 2024, a robust FEA software known for advanced material modelling and multiscale analysis.

The selection and development of the 3D RVE model were informed by methodologies presented in previous research (Barbero, 2013; Mobasher, 2012), ensuring consistency with established micromechanical modelling practices

3.4.2 Purpose of the model

The primary aim of the numerical simulation, despite available experimental results, was to extract the complete set of engineering constants for mango fibre reinforced concrete in all principal directions, including longitudinal and transverse elastic moduli, shear moduli, and Poisson's ratios. Simulation additively enabled comparative evaluation of the mechanical behaviour of mango fibre reinforced concrete and plain concrete using established failure theories, with validation performed against experimental results.

The Von Mises criterion was employed to model ductile failure under uniaxial compression, while the Maximum Principal Stress criterion was utilized to capture brittle fracture under uniaxial tension, in accordance with established practices in concrete failure analysis (Muthukumar, 2014).

3.4.3 Assumptions of mango fibre reinforced concrete model

i. Fibres are embedded in a semi-plastic mixture.
ii. Fibres are isotropic.
iii. Fibres and matrix are isotropic, but unidirectional fibre alignment causes anisotropic mechanical behaviour depending on load direction.

iv. Fibres are cylindrical and randomly distributed, forming a hexagonal microstructure arrangement (see Figure 3.12).

v. A strong interfacial bond exists between the fibre and the surrounding matrix.

vi. The short distance between the fibres and the matrix enhances load transfer.

3.4.3 Limitations of FEM assumptions

The FEM model was developed using simplifying assumptions to capture overall mechanical trends; however, these assumptions may idealize some local stress–strain behaviour and microstructural effects. The potential limitations of the assumptions outlined in Section 3.4.3 are presented below.

i. Fibres were assumed to be embedded in a semi-plastic mixture, which does not reflect local variations.

ii. Fibres were considered isotropic, whereas natural fibres exhibit some anisotropy.

iii. Although the matrix and fibres were treated as isotropic, unidirectional fibre alignment introduces anisotropic mechanical behaviour that may not be fully captured.

iv. Fibres were modelled as cylindrical and randomly distributed in a hexagonal microstructure thus idealizing the actual placement

v. A perfect bond was assumed between fibres and the surrounding matrix, while interfacial debonding or slip can occur under loading.

vi. The short fibre–matrix distance was assumed to enhance load transfer uniformly, which may overestimate stress bridging in regions with fibre clustering or voids.

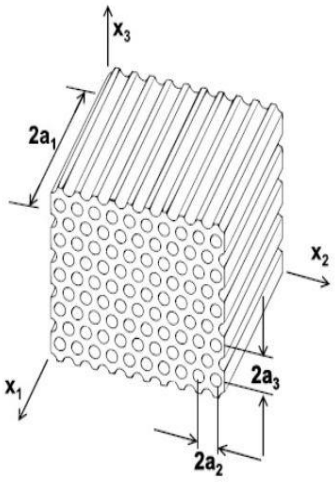

(k) Composite material arranged in a hexagonal fibre array

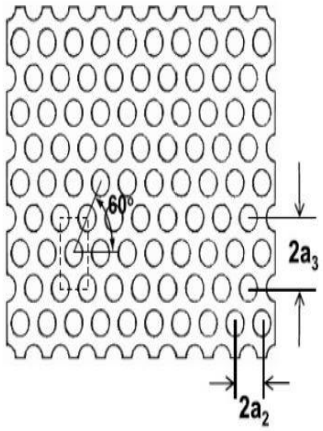

(l) Cross-sectional view of the composite

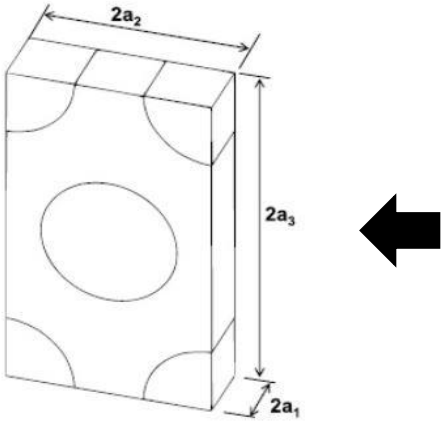

(n) 3D Representative Volume Element (3D RVE)

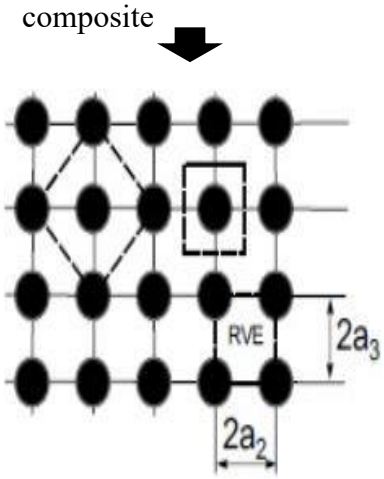

(m) Composite featuring a periodic square fibre arrangement

Figure 3.12 (k – n) Formation of a 3D RVE

(Barbero, 2013)

3.4.4 Determination of RVE size

i. Average fibre diameter = 66.83 µm

Volume fraction of fibres; $V_f = \frac{4a_1\Pi(\frac{d_f}{2})^2}{2a_1*2a_2*2a_3}$ (3.8)

Where: V_f = Volume fraction of fibres

: 4 = Number of fibres (or nodes) in the rectangular array, as shown in Figure 3.12 (m)

ii. The relationship between a_2 and a_3 was established by the hexagonal array pattern, for which $a_3 = a_2\tan 60°$ and $a_1 = \frac{a_2}{4}$ (Barbero, 2008).

iii. The optimal fibre content of 1.00% fibre content was selected to model the behaviour of the fibres in concrete, so $V_f = 1\%$

This implies that a_2 = 318.22 µm, a_3 = 551.17 µm and a_1 = 79.55 µm.

The dimensions of the RVE are detailed in Table 3.11;

Table 3.11 Size of Representative Volume Element

Fibre radius	V_f	**Hexagonal size of RVE, µm**		
(µm)		**$2a_1$**	**$2a_2$**	**$2a_3$**
33.42µm	0.01	159.10µm	636.44µm	1102.34µm
Converting from RVE geometry parameters from µm to mm				
0.03342mm	0.01	0.1591mm	0.6364mm	1.1023mm

3.4.5 Sketching model geometry

The RVE geometry, defined by dimensions $2a_1$, $2a_2$, and $2a_3$, was sketched in the Part module of ABAQUS using the Cartesian coordinate system, where $2a_1$, $2a_2$, and $2a_3$ correspond to the X-, Y-, and Z-directions, respectively. The RVE was modeled as a rectangular prism representing a periodic unit cell of a unidirectional fibre-reinforced composite.

Cylindrical fibres (radius = 33.42 mm) were embedded within the matrix and aligned along the Z-axis. The fibre layout included one fibre at the center and additional fibres positioned symmetrically near the edges of the X–Y plane, forming a periodic arrangement representative of square packing as illustrated in Figure 3.12 (n).

The surrounding volume was designated as the matrix phase, and the overall geometry, maintained symmetry and periodicity in all directions to facilitate the application of periodic or constraint-based boundary conditions during homogenization.

3.4.6 Material properties definition

Assuming linear elastic behaviour, the mechanical response of the material along its principal directions was characterized using a set of engineering constants, including the elastic moduli (E_{11}, E_{22}, E_{33}), Poisson's ratios (ν_{12}, ν_{13}, ν_{23}), and shear moduli (G_{12}, G_{13}, G_{23}). Two approaches are commonly used to compute the aforementioned elastic properties:

a) Computational micromechanics using periodicity (periodic boundary conditions) and python scripting in ABAQUS and/ or,

b) Computational micromechanics modeling in ABAQUS employing tie constraints and master-slave nodal coupling (Barbero, 2013).

For this study, the engineering constants were derived using the periodic micromechanics method (PMMIE), corresponding to option (b).

ABAQUS CAE 2024 did not have a direct field to enter a concrete grade and was therefore translated into material properties. The typical inputs for material properties for concrete were elastic properties and; plasticity and damage behaviour parameters defined by Concrete Damaged Plasticity

a) Elastic properties

Young's modulus was estimated based on characteristic compressive strength

From BS EN 1992-1-1:2004, the approximate relation for Young's modulus is given by equation 3.9:

$$E = 22 \times \left(\frac{f_{cm}}{10}\right)^{0.3} \tag{3.9}$$

Where; $f_{cm} = f_{ck} + 8$ MPa (3.10)

Poisson's ratio, v, for normal concrete is typically about 0.2 – 0.25. For this research, $v = 0.2$

The tensile strength, $f_{ctm,}$ was obtained from the experimental laboratory results. i.e., $f_{ctm} = 2.7$ MPa and was used to define tensile behaviour in Concrete Damaged Property as illustrated in Table 3.13.

The material properties for ABAQUS models and extracted engineering constants were summarized in Table 3.12:

Table 3.12 Model parameters.

PMMIE, isotropic fibre, elastic matrix							
Fibre content	1.00%		1.50%				
Matrix concrete	Elastic modulus, E_m (MPa)					31,600 MPa	
	Poisson's ratio, v_m					0.2	
Mango fibres	Elastic modulus, E_f (MPa)					3,420 MPa	
	Poisson's ratio, v_f					0.3	
Extracted Engineering constants							
Fibre content	E_1 (MPa)	E_2 (MPa)	E_3 (MPa)	$v_{12} = v_{13}$	v_{23}	$G_{12} = G_{13}$ (MPa)	G_{23} (MPa)
1.00%	30000	28000	27000	0.25	0.3	15000	14000

Where; -

$$E = \frac{\sigma}{\varepsilon} \tag{3.11}$$

$$v = \frac{\varepsilon_x}{\varepsilon_y} \tag{3.12}$$

$$G = \frac{E}{[2\times(1+V)]} \tag{3.13}$$

σ = Stress, ε = strain, ν = Poisson's ratio

G_{12} = in-plane shear modulus/ transverse shear modulus/ shear modulus in XY plane, G_{13} = interlaminar shear modulus/ longitudinal shear modulus/ shear modulus in XZ plane, G_{23} = shear modulus in YZ plane

ν_{12} = Transverse strain in Y due to uniaxial strain in X, ν_{13} = Transverse strain in Z due to uniaxial strain in X, ν_{23} = Transverse strain in Z due to uniaxial strain in Y

For a hexagonal array of fibres $G_{12} = G_{23}$

(Barbero, 2013)

The nonlinear behaviour of the material was characterized using the Concrete Damaged Plasticity (CDP) model. The plasticity parameters, along with the compression and tensile behaviour inputs for the CDP model, are detailed in Table 3.13:

Table 3.13: Compression and Tension behaviour parameters

Concrete Damaged Plasticity				
Plasticity				
Dilation Angle	Eccentricity	fb0/ fc0	K	Viscosity parameter
40	0.1	1.16	0.6667	0.002
Compression behaviour		**Tension behaviour**		
Yield stress (N/mm)	Inelastic strain (dimensionless)	Yield stress (N/mm)	Inelastic strain (dimensionless)	
30.5	0	2.7	0	
34	0.00067	2.2	0.00013	
29.8	0.00157	1.7	0.00036	
25	0.0026	1.45	0.00048	
20.5	0.0036	1.15	0.0006	
16.3	0.00455	0.8	0.00092	
13.2	0.00546	0.5	0.00115	
11	0.00614			

3.4.6 Section assignment

After defining the material properties for the RVE, the next step involved assigning sections to the distinct components of the RVE geometry within ABAQUS. The fibre regions were assigned the fibre material properties, while the surrounding matrix volume

was assigned the matrix material properties. This differentiation ensured that each phase of the composite responded according to its respective constitutive behaviour during the simulation.

3.4.7 Assembly definition

After section assignment, the fibre and matrix components of the RVE were combined to create a single, unified model representing the complete representative volume element. Within the Assembly module, an Independent Instance was selected to facilitate the application of tie constraints and periodic boundary conditions.

3.4.8 Step definition

Two distinct analysis steps were defined based on the intended simulation objectives.

For the linear elastic analysis, aimed at extracting effective engineering constants such as elastic moduli, Poisson's ratios, and shear moduli, a Static General step under small displacement assumptions was defined.

In contrast, to capture nonlinear behaviour and failure mechanisms, two separate Static General steps were created: one for uniaxial compression and another for uniaxial tension - each incorporating the Concrete Damaged Plasticity (CDP) model. These steps enabled displacement-controlled loading which was necessary for extracting failure-related outputs such as, Von Mises stress and maximum principal stress, with their corresponding failure loads.

3.4.7 Definition of boundary conditions

Boundary conditions were defined within the Load module using the Boundary Condition Manager. Both Symmetry/Anisotropic/Encastre and Displacement/Rotation boundary types were applied. Symmetry boundary conditions were assigned to the RVE faces normal to the X- and Z-axes, while displacement constraints were applied to the bottom and loaded faces.

The bottom face was fully constrained (U2 = U3 = 0), while the loaded face was prescribed U2 = 0 and U3 = $2a_1$ (i.e., the full RVE height) to satisfy periodicity and enable the extraction of engineering constants.

For failure analysis, the displacement on the loaded face in the Z-direction (U3) was incrementally varied (0.25, 0.50, 0.75, and 1.0) to simulate progressive uniaxial loading.

3.4.8 Tie constraints

After assigning boundary conditions, tie constraints were applied to the node regions of the RVE rather than only on the surfaces to enforce pure shear. This process resulted in the creation of two additional sets: m_Set-4 and s_Set-4. m_Set-4. These were subsequently renamed to RVE_Front_Face whereas s_Set-4 was renamed to RVE_Back_Face respectively. The distance between the master and slave surfaces corresponded to $2a_1$; which represents the thickness of the RVE.

3.4.9 Meshing and element type

After applying tie constraints, the RVE geometry was discretized using a structured mesh of hexahedral elements with reduced integration. Hexahedral elements were selected due to their suitability for structured meshing and periodic boundary conditions, as well as their effectiveness in capturing interfacial stresses within fibre–matrix composites.

Linear 8-node hexahedral elements (C3D8) were employed to strike a balance between computational efficiency and accuracy for linear elastic analyses. Although quadratic elements (C3D20) provide higher accuracy, their computational demands exceeded the available workstation capacity.

A global mesh size of 15 μm was adopted to ensure an optimal balance between computational efficiency and mesh resolution, considering the processing capabilities of the workstation.

3.4.9 Solution

A Python script was executed within the ABAQUS CAE Python shell to extract the elastic properties and failure load results of the composite. The extracted data are presented in the Tables 3.13 and 4.9.

3.4.10 Model validation

Model validation was carried out by comparing FEM-predicted tensile and compressive strengths with experimental values for plain concrete and MFRC. Quantitative accuracy

indicators; percentage error and absolute deviation, were computed to assess model reliability.

To obtain these validation results, the following procedure was followed. Peak tensile and compressive stresses were first extracted from the FEM simulations based on the maximum stress recorded in the UTS and UCS analyses for each material system. These peak stresses were taken as the FEM-predicted strengths. The corresponding experimental strengths were then compiled for direct comparison.

For each material type, the difference between FEM-predicted and experimental strengths was evaluated using two numerical accuracy measures. The percentage error was computed using equation 3.14:

$$Percentage\ Error = \frac{|f_{FEM} - f_{exp}|}{f_{FEM}} \times 100 \tag{3.14}$$

While the absolute deviation was computed using equation 3.15:

$$Absolute\ Deviation = |f_{FEM} - f_{exp}| \tag{3.15}$$

Where; - f_{FEM} – simulated or predicted value and, f_{exp} – experimental value

The detailed numerical validation results are presented in Chapter 4.

CHAPTER FOUR: RESULTS AND DISCUSSION

4.1 Introduction.

This chapter presents the experimental findings on the influence of mango fibres on the structural performance of concrete. For accurate interpretation and description of data, statistical techniques were applied so as to generate meaningful insights. Scanning Electron Microscope (SEM) imagery was used to examine the morphological characteristics of the samples, while ABAQUS finite element software was employed to analyze the 3D Representative Volume Element (RVE) model.

4.2 Presentation and analysis of results.

4.2.1 Geometric, physical and strength properties of mango fibres.

Table 4.1 presents a summary of geometric, physical and strength properties of mango fibres that were generated with the aid of a Tescan Vega 3 SEM, a YG003E Single fibre strength tester, FY2027B stiffness tester, precision balance and steel meter ruler. The Laboratory test results on the mango fibres are presented in Appendix C2

Table 4.1 Geometrical, physical, and mechanical properties of mango fibres

Fibre parameter	Untreated mango fibres	Treated mango fibres
Stiffness (mm)	3.2 mm	2.3 mm
Linear density (g/cm^3)	23.08 g/cm^3	15.52 g/cm^3
Diameter (μm)	81.48 μm	66.83 μm

Table 4.1 Continued

Breaking force (cN)	143.68 cN	216.43 cN
Breaking elongation (%)	2.3 %	3.8 %
Tensile strength (MPa)	275.57 MPa	616.96 MPa

From Table 4.1, the treated mango fibres exhibited improved strength, which agreed with earlier studies showing that alkali treatment enhances the performance of natural fibres (Yimer and Gebre, 2023; Habibi et al., 2023; Adekunle, 2015). Accordingly, a caustic soda solution was used in this study, and the treated fibres were incorporated into the plain concrete.

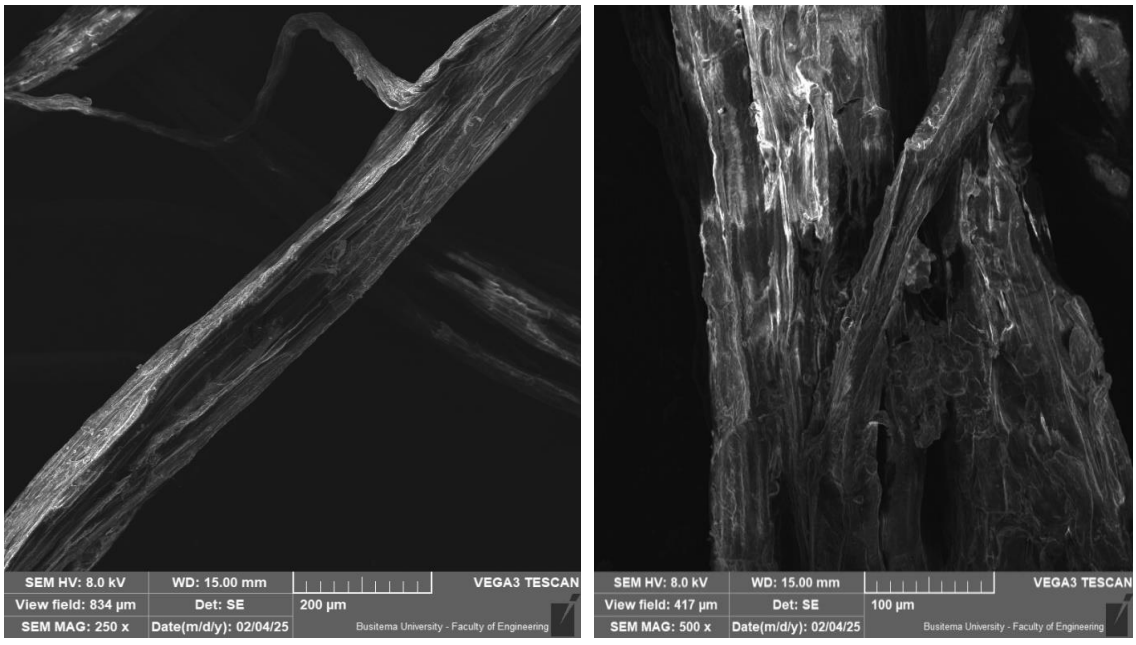

Figure 4.1 SEM Micrographs

Figure 4.1 shows images of Scanning Electron Micrographs for mango fibres. Treated mango fibres had not a smooth but rather rough surfaces which helped them bond with

concrete. The Tescan Vega 3 SEM provided the individual diameter of each mango fibre and calculated the average fibre diameter that was used during this research.

4.2.2 Chemical and physical composition for CEM 1 (42.5N)

Chemical and physical test certificates for CEM 1 (42.5N) were provided by Tororo cement limited (Manufacturer) on purchase of cement and were summarized in the Tables 4.2 and 4.3. The test certificate was attached in Appendix C3

Table 4.2 Chemical analysis on CEM I (42.5N), Tororo cement – OPC

Parameter	Specification	Composition (%)
Sulphuric Anhydride (SO_3)	MAX: 3.50	1.70
Chloride	MAX: 0.10	0.007
L.O. I	MAX: 5.0	1.89
I.R	MAX: 5.0	0.56
Total Alkali Na equalent	NR	0.567
Al_2O_3	MAX: 3.50	4.37
Fe_2O_3	-	4.21
CaO	-	64.17
MgO	MAX: 3.0	1.36
Na_2O	-	0.33
K_2O	-	0.36
C_3A	-	4.457

The chemical composition of the CEM I (42.5N) cement met the required standards. The SO_3 (1.70%) and chloride (0.007%) contents were well below their limits, while the LOI (1.89%) and insoluble residue (0.56%) remained within acceptable ranges. The main oxides; CaO (64.17%), Al_2O_3 (4.37%) and Fe_2O_3 (4.21%), were typical of OPC, and the MgO content (1.36%) was sufficiently low to avoid unsoundness. The C_3A (4.457%) and alkali equivalent (0.567%) were moderate, indicating stable hydration and low ASR risk. Overall, the chemical results showed that the cement was suitable for structural concrete.

Table 4.3 Physical test results on CEM I (42.5N), Tororo cement – OPC

Test Item	**Specification**	**Unit**	**Findings**
Fineness (Blaine)	NR	m^2/kg	345.6
Setting Time			
a) Initial	MIN: 60	minutes	150
b) Final	MAX: 600	minutes	240
Soundness by Lechatilier	MAX 10.0	mm	0.0
Compressive strength			
a) 48 ± 1 hour	MIN; 10.0	MPa	18.95
b) 168 ± 2 hours	NR	MPa	31.74
c) 672 ± 4 hours	MIN 42.5	MPa	45.86

The physical test results showed that the CEM I (42.5N) cement met the required performance standards. Its fineness (345.6 m^2/kg) indicated adequate grinding, while the initial and final setting times (150 and 240 minutes) fell within acceptable limits. The soundness value of 0.0 mm confirmed good volumetric stability. The compressive strengths at 48, 168, and 672 hours (18.95, 31.74, and 45.86 MPa) satisfied the strength

requirements for the 42.5N class. Overall, the cement demonstrated appropriate setting behaviour, stability, and strength development for structural applications.

4.2.3 Results on coarse and fine aggregates

The physical properties that were looked at are; aggregate type, sieve analysis, unit weight, specific gravity, water absorption and gradation and these were findings presented in tables as follows;

4.2.3.1 Gradation of coarse aggregates

Gradation analysis of the coarse aggregates was carried out to determine their particle size distribution and assess their conformity with the recommended grading limits for concrete production. The gradation of coarse aggregates plays a critical role in influencing workability, compaction, and the interlocking behaviour of particles within the concrete matrix. A well-graded coarse aggregate system improves load transfer, reduces the paste requirement, and minimizes segregation and bleeding, thereby contributing to enhanced mechanical strength and long-term durability of the concrete. The particle size distribution obtained in this study is shown in Figure 4.2, and the grading characteristics assessed in this section evaluate the suitability of the coarse aggregates for the concrete mixes used

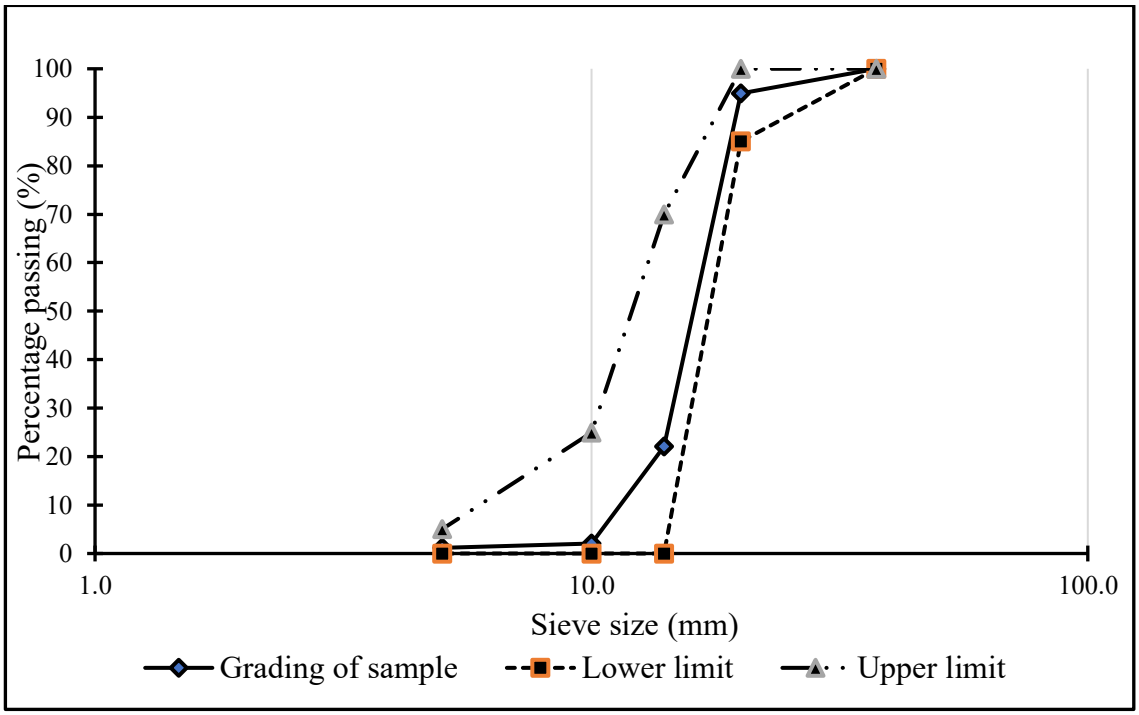

Figure 4.2 Percentage passing (%) against sieve sizes (mm)

4.2.3.2 Gradation of fine aggregates

Gradation analysis was conducted to evaluate the particle size distribution of the fine aggregates and to determine their compliance with the grading limits specified for concrete production. Proper gradation is essential because it affects workability, compaction, and the overall packing efficiency of the aggregate system, which in turn influences the strength and durability of the hardened concrete. Well-graded fine aggregates enhance cohesion within the mix, reduce void content, and contribute to improved mechanical performance. The results presented in Figure 4.3 exhibit the grading profile of the fine aggregates and assess their suitability for the concrete mixtures used in this study.

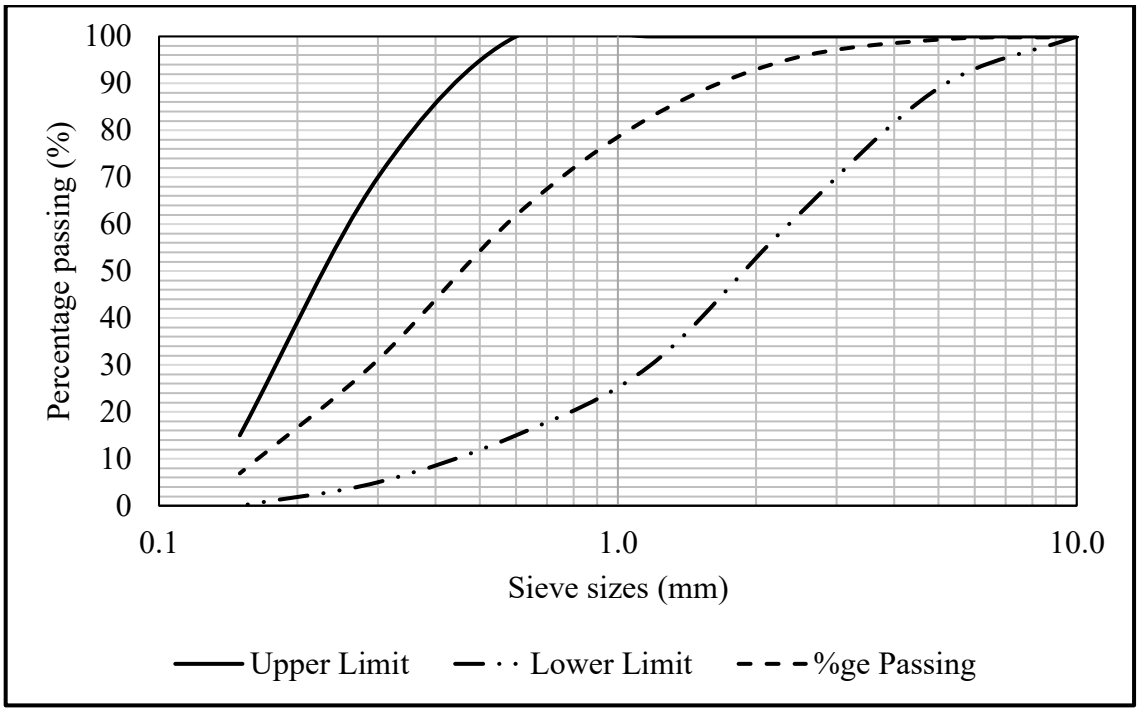

Figure 4.3 Percentage passing against sieve sizes

A coarse-grained soil is considered well graded when it contains a wide and balanced distribution of particle sizes, with no significant excess or deficiency in any particular range. This ensures good interlocking and packing density. In contrast, a poorly graded soil lacks this diversity. It may consist predominantly of particles within a narrow size range, referred to as uniformly graded, or it may contain both fine and coarse particles but lack a sufficient amount of intermediate-sized particles, a condition known as gap grading or step grading (Knappett and Craig, 2012; Whitlow, 1995).

A well-graded soil typically produces a smooth, continuous gradation curve on a particle size distribution graph, indicating a wide range of particle sizes. In contrast, a poorly

graded soil is represented by a steep or irregular curve, reflecting a limited range of particle sizes or missing intermediate sizes (Whitlow, 1995).

From Figure 3.8, we can deduce that the sand used for this experimental program was well graded since the slope for the percentage passing envelope was smooth. Notably, a quantitative analysis can be carried for which; the particle size at which 10% of the soil sample is finer is referred to as D_{10} which is commonly referred to effective size (Knappett and Craig, 2012). Similarly, D_{30} and D_{60}, represent the sizes at which 30% and 60% of the particles are finer, respectively. The effective size, D_{10}, particularly important, as it is often used in empirical correlations to estimate the permeability of the soil (Whitlow, 1995). From Figure 3.8, D_{10} = 0.18 mm, D_{30} = 0.3 mm and, D_{60} = 0.58 mm

The overall gradient and form of the particle size distribution curve can be characterized using two key parameters: the coefficient of uniformity (C_u) and the coefficient of curvature (C_c or C_z). These are calculated using the following expressions:

$$C_u = \frac{D_{60}}{D_{30}} \tag{4.1}$$

$$C_z = \frac{D^{2}30}{D_{60}D_{10}} \tag{4.2}$$

A soil is generally considered well-graded if its coefficient of curvature (Cc) lies between 1 and 3, indicating a balanced distribution of particle sizes (Knappett and Craig, 2012; Whitlow, 1995). This further proves that the fine aggregates (sand) used for this experimental test program were well graded since the value for coefficient of uniformity, C_u = 1.9333 was between 1 and 3.

Table 4.4 Physical properties of coarse and fine aggregates

Test item	Findings	Allowable
Rodded bulk density (fine aggregates)	1583 kg/m^3	1400 – 1700 kg/m^3
Loose bulk density (fine aggregates)	1285 kg/m^3	1200 – 1500 kg/m^3
Rodded bulk density (coarse aggregates	1516 kg/m^3	1450 – 1700 kg/m^3
Loose bulk density (coarse aggregates)	1290 kg/m^3	1200 – 1500 kg/m^3
Flakiness Index (Coarse aggregates)	16.1%	<25 – 30%
Elongation Index (Coarse aggregates)	0%	<15 – 20%
Average Impact Value (AIV) Test	20.6	$\leq$ 30%
Average silt content in Sand	3.0%	< 6%
Specific gravity (Fine aggregates)	2617 kg/m^3	N/A
Water absorption (Fine aggregates)	0.963%	$\leq$ 2%
Specific gravity (Coarse aggregates)	2637 kg/m^3	2.5 – 2.7
Water absorption (Coarse aggregates)	0.235%	$\leq$ 3%

4.2.4 Compressive strength test

4.2.4.1 Compressive strength at 7 days

Figure 4.4 presents the effect of varying fibre content and length on the compressive strength samples containing plain concrete (reference concrete) and Mango fibre reinforced concrete at 7 days.

Test results for fibre length (30, 40 and 50 mm) and the corresponding fibre content (0.1%, 0.25%, 1.0% and 1.5%) are presented in Appendix C4. Appendix C4 further shows the following parameters; mean strength, minimum and maximum strength; standard deviation, Coefficient of variation, Correlation coefficients, T-statistics and P-Value for both plain concrete and MFRC. The following observations were drawn:

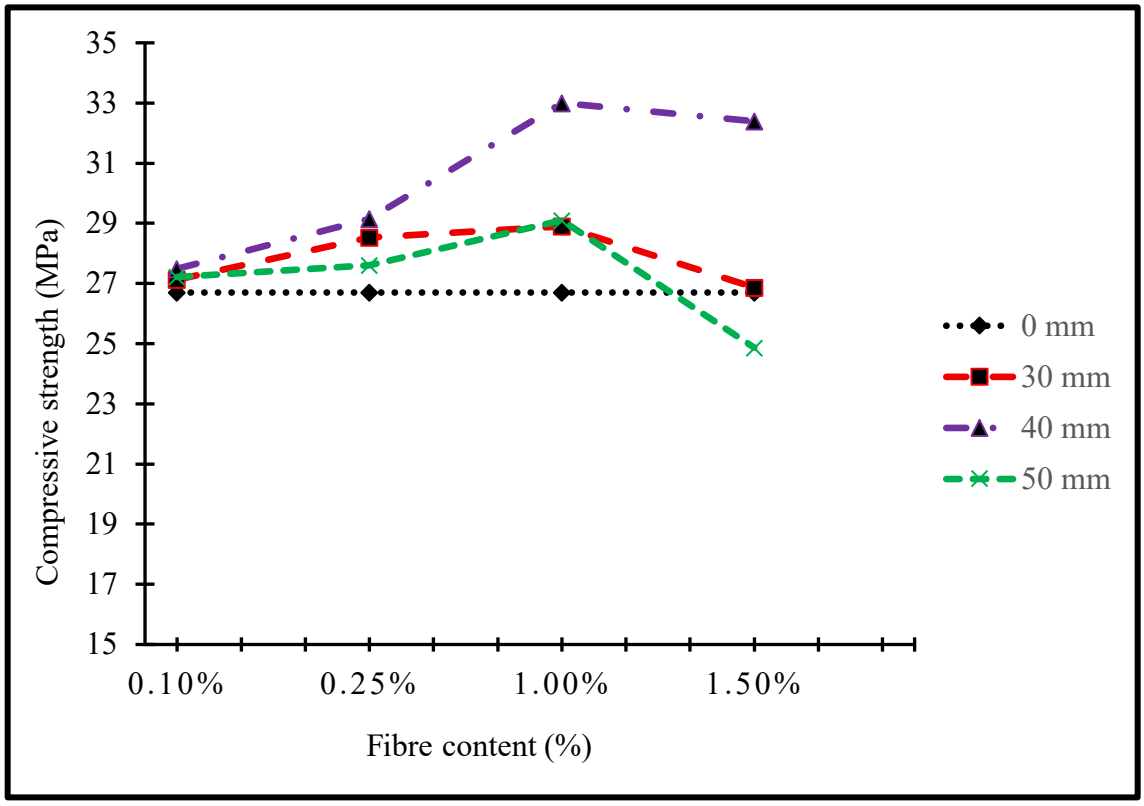

Figure 4.4 Effect of fibre content on compressive strength in concrete at 7-days

From Figure 4.4, for 30mm and 40 mm fibre lengths, at all fibre contents, the mean compressive strength of MFRC was higher than that of the reference (plain) concrete.

For 50mm, with a corresponding fibre content 0.1%, 0.25% and 1.0%, the mean compressive strength of MFRC was higher than that of the plain concrete but at 1.5% fibre content, the mean compressive strength of MFRC was lower than that of the plain concrete.

The mean compressive strength increased by 8.2% for 30 mm fibre length, by 23.6% for 40 mm fibre length and by 9% for 50mm fibre length as mango fibre content was increased from 0.1% to 1.0% in comparison to plain (reference) concrete.

However, the corresponding *p*-values exceeded 0.05, indicating that these early-age improvements were not statistically significant. This suggests that while fibres may contribute to early strength gain through crack-bridging and stress redistribution, the variation among samples limits statistical confirmation.

4.2.4.2 Compressive strength at 28 days

Figure 4.5 presents the effect of varying fibre content and length on the compressive strength samples containing plain concrete (reference concrete) and Mango fibre reinforced concrete at 28 days.

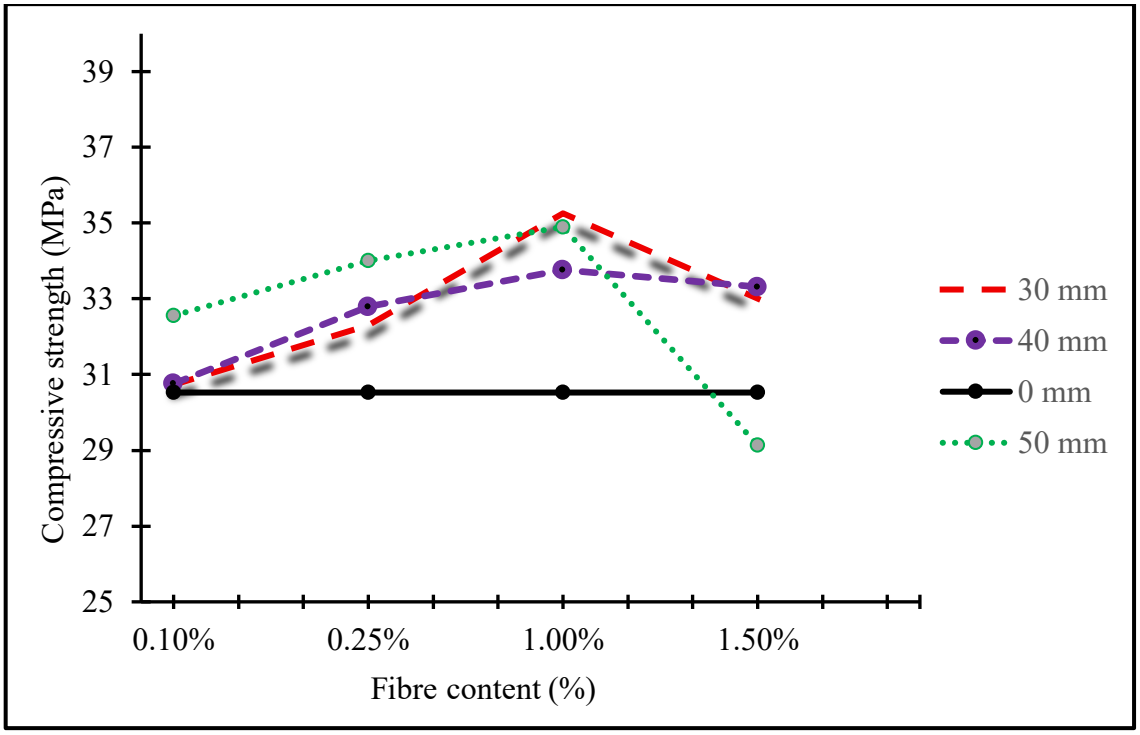

Figure 4.5 Effect of fibre content on compressive strength in concrete at 28-days

Test results for fibre length (30, 40 and 50 mm) and the corresponding fibre content (0.1%, 0.25%, 1.0% and 1.5%) are presented in Appendix C4. Appendix C4 further shows the following parameters; mean strength, minimum and maximum strength; standard deviation, Coefficient of variation, Correlation coefficients, T-statistics and P-Value for both plain concrete and MFRC. The following observations were drawn; -

The mean compressive strength increased by 15.7% for 30 mm fibre length, by 10.8% for 40 mm fibre length and by 14.4% for 50mm fibre length as mango fibre content was increased from 0.1% to 1.0% in comparison to plain concrete.

Nonetheless, the computed *p*-values were still greater than 0.05, signifying that the improvements were not statistically significant at the 95% confidence level. The observed increases are therefore considered practically meaningful but not statistically proven.

Conclusively, both 7- and 28-day results demonstrate a consistent positive trend in compressive strength with fibre inclusion, aligning with the reinforcing mechanisms reported in prior studies (Younis, 2016; Elbehiry et al., 2020).

The mean compressive strength attained for MFRC was higher than that of plain concrete as fibre content increased from 0.1% to 1% for all fibre lengths and for both 7- and 28-day tests. This improvement is attributed to the reinforcing action of mango fibres, where the fibres bridge micro-cracks and share part of the compressive load with the cementitious matrix, enhancing stress redistribution and delaying crack propagation (Zhang et Al., 2018). Similar findings on compressive strength reported by (Dhawan et Al., 2021) and (Elbehiry et Al., 2020), supporting the observed trend that natural fibres

improve load transfer efficiency and toughness under compression. Mechanistically, the fibres transferred tensile stress across micro-cracks, delaying failure and improving the composite's compressive toughness.

The reduction in mean compressive strength despite a further addition of fibre content beyond 1.0% for all fibre lengths can be attributed to the balling effect which occurred as a result of manual inclusion of fibres at the time of mixing leading to non-uniform distribution within the mix and to the increased air-void content at higher fibre volumes, which disrupts the concrete matrix and reduces effective load-bearing area (Yimer and Gebre, 2023; Zhang et Al., 2018); (Younis, 2016) similarly reported that excessive fibre addition increases porosity, counteracting the reinforcing benefit due to stress localization which initiates premature crushing.

Compared with other natural fibres, the compressive strength of Mango Fibre Reinforced Concrete at optimal content falls within the same improvement range reported for Banana and Sisal Fibre Reinforced Concrete (Dhawan et Al., 2021; Karubanga et Al., 2021; Elbehiry et Al., 2020; Prasannan et Al., 2018).

4.2.5 Flexural strength test

For this experimental study, flexural strengths for both plain (reference) concrete and Mango Fibre Reinforced concrete were determined.

Figure 4.6 presents the effect of varying fibre content and length on flexural strengths for both plain and Mango Fibre Reinforced concrete at 28 days.

Test results for fibre length (30, 40 and 50 mm) and the corresponding fibre content (0.1%, 0.25%, 1.0% and 1.5%) are presented in Appendix C6. Appendix C6 further shows the following parameters; mean strength, minimum and maximum strength; standard deviation, Coefficient of variation, Correlation coefficients, T-statistics and P-Value for both plain concrete and MFRC. The following observations and conclusions were drawn:

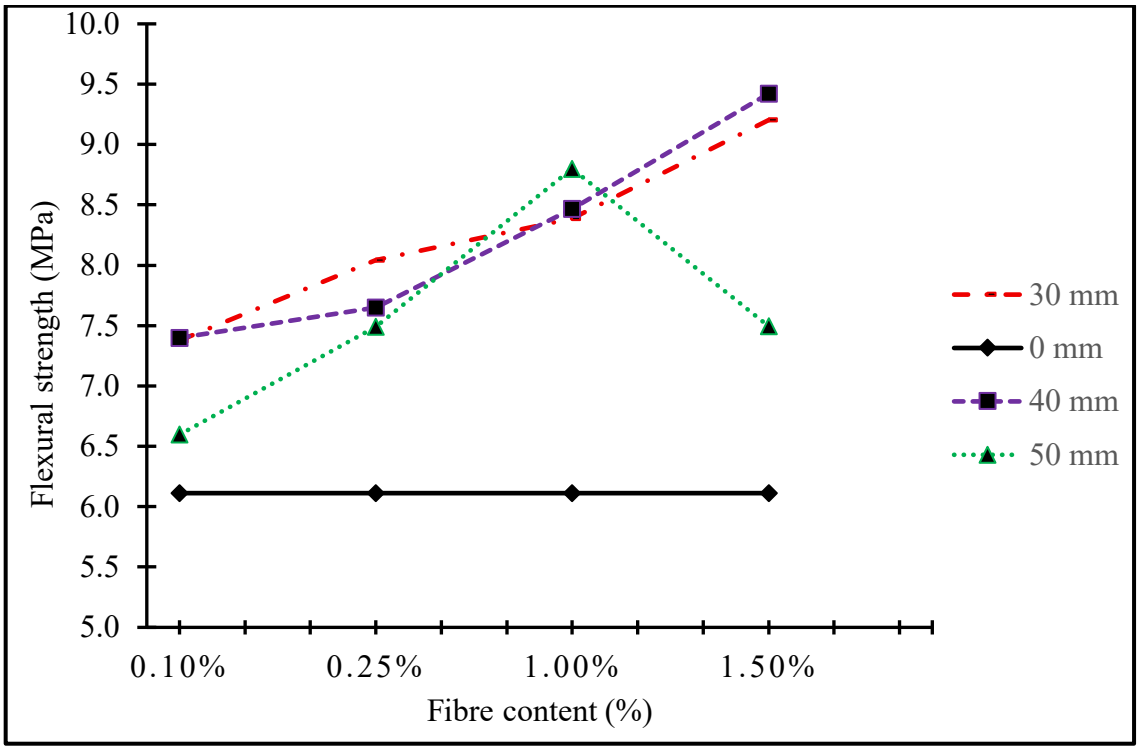

Figure 4.6 Effect of fibre content on flexural strength in concrete at 28-days

It was observed that the flexural strengths for all fibre contents and lengths were higher than those of plain (reference) concrete. For fibre lengths, 30mm and 40mm, it was observed that the flexural strengths increased with increase in fibre content. The mean flexural strength increased by 50.8% for 30 mm fibre length and by 54.1% for 40 mm

fibre length as fibre content was increased from 0.1% to 1.0% in comparison to plain concrete.

The findings for the correlation coefficient exhibited a strong positive correlation which implied that increase in fibre content and length implies an increase in flexural strength. Conversely, the coefficient of variation for these fibre lengths (30 and 40 mm) implied that the data points were moderately dispersed about the mean which indicated moderate variability. Despite this, all *p*-values obtained were greater than 0.05, indicating that these differences were not statistically significant at the 95% confidence level.

For fibre length 50 mm, it was observed that flexural strength increased with increasing fibre content up to 1.0% beyond which it reduced. The mean flexural strength increased by 44.3% for 50mm fibre length as fibre content was increased from 0.1% to 1.0% in comparison to plain concrete.

From the findings of the correlation coefficient, the degree of correlation between fibre content and length 50 mm was moderate and, the coefficient of variation exhibited that the data points were moderately dispersed about the mean which indicated moderate variability.

The results for flexural strength revealed both an increase and reduction in the strength obtained at 28 days. The increase in flexural strength of MFRC can be attributed to the effective stress transfer between the cement matrix and mango fibre, whose bridging capability delayed the propagation of micro-cracks enhancing post-cracking load-carrying

capacity. This mechanism delays crack propagation and improves the composites ductility (Younis, 2016; Mobasher, 2012).

Conversely, at higher fibre contents and length, the flexural strength decreased due to fibre agglomeration which occurred as a result of manual inclusion of fibres at the time of mixing which introduced voids and weak zones that disrupted the continuity of the matrix and reduced interfacial bonding efficiency. The resulting reduction in effective cross-sectional area and non-uniform stress distribution led to premature crack initiation (Yimer and Gebre, 2023; Zhang et Al., 2018; Younis, 2016).

These trends align with findings from (Prasannan et Al., 2018; Elbehiry et Al., 2020; Dhawan et Al., 2021; Karubanga et Al., 2021), confirming that natural fibre reinforcement exhibits an optimum dosage range beyond which mechanical performance deteriorates due to reduced compaction quality and increased porosity.

4.2.6 Split tensile strength test

For this experimental study, split tensile strengths for both plain (reference) concrete and Mango Fibre Reinforced concrete were determined. Figure 4.7 presents the effect of varying fibre content and length on split tensile strengths for both plain and Mango Fibre Reinforced concrete at 28 days. Test results for fibre length (30, 40 and 50 mm) and the corresponding fibre content (0.1%, 0.25%, 1.0% and 1.5%) are presented in Appendix C5. Appendix C5 further shows the following parameters; mean strength, minimum and maximum strength; standard deviation, Coefficient of variation, Correlation coefficients, T-statistics and P-Value for both plain concrete and MFRC.

The following observations and conclusions were drawn; -

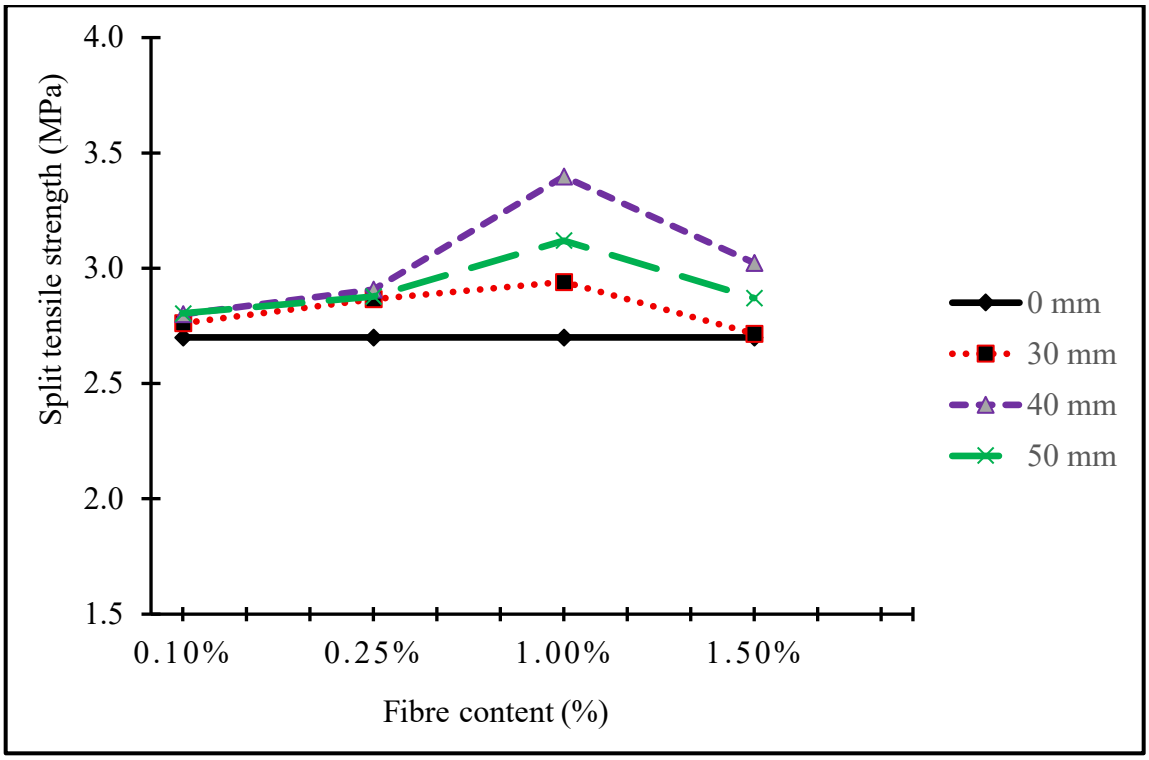

Figure 4.7 Effect of fibre content on split tensile strength in concrete at 28-days

For all fibre lengths and contents, it was observed that the mean split tensile strength of MFRC was higher than that of the reference (plain) concrete. The split tensile strengths for all fibre contents and lengths increased up to 1.0% beyond which a reduction in strength was observed.

The mean split tensile strength increased by 7.4% for 30 mm fibre length, by 25.9% for 40 mm fibre length and by 14.8% for 50mm fibre length as fibre content was increased from 0.1% to 1.0% in comparison to plain concrete.

There was a general indirect correlation between fibre content and length and, split tensile strength for the 30 mm fibre length. The coefficient of variation was low implying that the data points were closely clustered around the mean which indicated high precision.

On the contrary, for 40 mm and 50 mm fibre lengths, there was a strong positive correlation between fibre content and length and, split tensile strength but the coefficient of variation was moderate which implied that the data points were moderately dispersed about the mean which indicated moderate variability.

Statistical analysis using two-sample *t*-tests showed that the corresponding *p*-values were above 0.05, which indicated no statistically significant difference between mango fibre reinforced concrete and plain concrete at $\alpha = 0.05$.

The results for split tensile strength revealed both an increase and reduction in the strength obtained at 28 days. The increase in flexural strength of MFRC can be attributed to due to the bridging capability of fibres that inertly delayed the propagation of tensile induced cracks (Younis, 2016; Mobasher, 2012). The fibres act as micro-reinforcement, bridging the crack faces and transferring tensile stresses across them, thereby enhancing tensile load-carrying capacity, post-cracking ductility, and energy absorption. Similar findings were reported by Dhawan et al. (2021) and Elbehiry et al. (2020), who observed strength improvements of 6–28% in natural fibre-reinforced concretes at optimal fibre contents, validating the trend observed in this study.

On the contrary, the reduction in split tensile strength despite an increment in fibre content and length can be attributed to the effect of increased porosity due to high air voids

contents and, balling effect which occurred as a result of manual inclusion of fibres at the time of mixing leading to non-uniform fibre distribution within the matrix (Yimer and Gebre, 2023; Zhang et Al., 2018; Younis, 2016). Mechanically, these regions serve as crack initiation points, reducing overall tensile capacity.

Comparable strength reductions at higher fibre dosages were similarly noted by (Prasannan et Al., 2018; Elbehiry et Al., 2020; Dhawan et Al., 2021; Karubanga et Al., 2021), for steel, sisal and banana fibres, reinforcing the conclusion that excessive fibre addition compromises tensile performance due to poor dispersion and increased porosity.

4.2.7 Drying shrinkage test

For this experimental study, drying shrinkage for both plain (reference) concrete and Mango Fibre Reinforced concrete were determined.

Figure 4.8 presents the effect of varying fibre content and length on drying shrinkage for both plain and Mango Fibre Reinforced concrete at 28 days.

Test results for fibre length (30, 40 and 50 mm) and the corresponding fibre content (0.1%, 0.25%, 1.0% and 1.5%) are presented in Appendix C7. Appendix C7 further shows the following parameters; mean strength, minimum and maximum strength; standard deviation, Coefficient of variation, Correlation coefficients, T-statistics and P-Value for both plain concrete and MFRC.

The following observations and conclusions were drawn; -

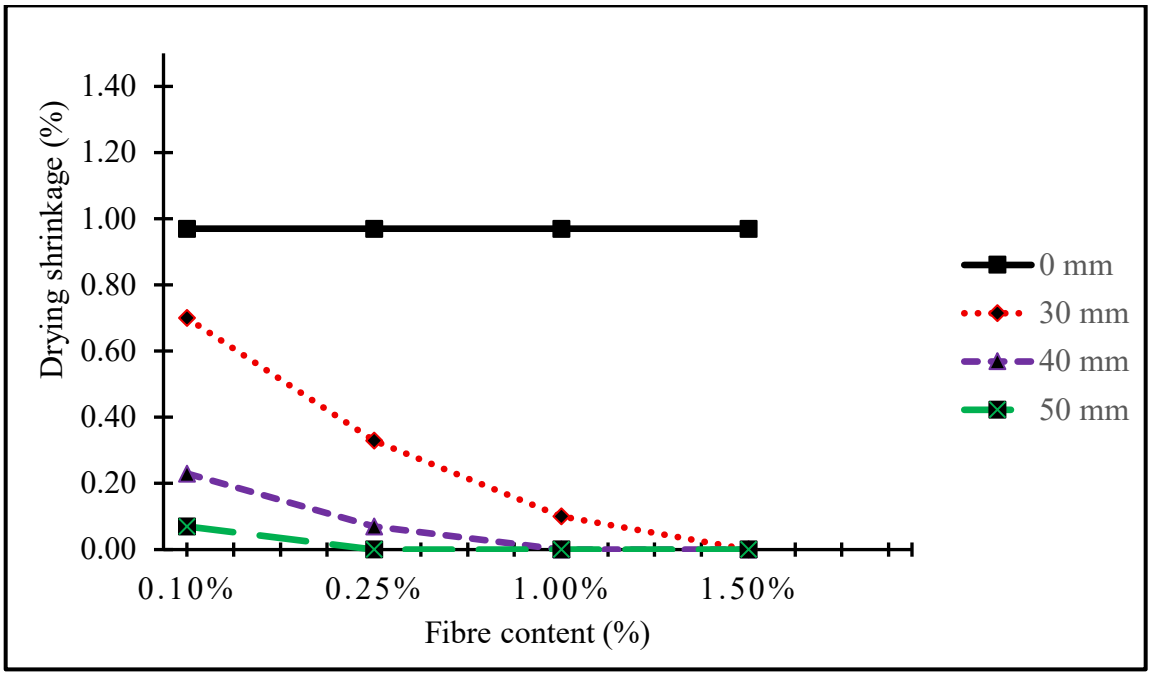

Figure 4.8 Effect of fibre content on drying shrinkage in concrete at 28-days

From Figure 4.8, it was observed that fibre content and length greatly reduced drying shrinkage in concrete. For all fibre contents and lengths, drying shrinkage in MFRC was lesser than that of plain concrete.

For 30 mm fibre length, as fibre content was increased from 0.1% to 1.5%, drying shrinkage reduced to zero and to zero, for 40 mm fibre length, as soon as fibre content was increased to 1.0% and to zero, for 50mm fibre length, as soon as fibre content was increased to 0.25%.

Statistical testing of the drying shrinkage data indicated a noticeable reduction in shrinkage strain with increasing fibre content. For the 30 mm fibre length, the *p*-value was approximately equal to 0.05, indicating a borderline statistically significant reduction in shrinkage compared to plain concrete. For the 40 mm and 50 mm fibre lengths, *p*-values

were slightly higher ($p > 0.05$) but still demonstrated the same trend of reduced shrinkage. These results provide statistical evidence that mango fibres contribute to controlling shrinkage, most effectively at moderate fibre lengths and contents.

An indirect correlation was observed between fibre content, fibre length, and drying shrinkage, while the relatively high coefficients of variation indicated that the data points were widely dispersed around the mean, suggesting considerable variability within the results.

The reduction in drying shrinkage in concrete can be attributed to crack-bridging capability of fibres which helps to distribute stresses and restricting crack or fracture development. The minimal to zero drying shrinkage crack test results can be attributed to the increase in fibre content and volume which enhances the mechanical qualities of concrete to resist fracture development (Eisa et Al., 2021; George et Al., 2021; Johny, 2022; Kim and Park, 2024). Mechanistically, the fibres act as internal reinforcement, transferring tensile stresses across potential micro-cracks and effectively reducing stress concentration points, thereby limiting shrinkage-induced damage.

Moreover, the ability of the fibres to restrain volume changes limits the development of tensile stresses that typically lead to shrinkage cracking. This behaviour is particularly significant in natural fibre-reinforced concrete, where the interfacial bonding between the fibre and matrix provides additional resistance to shrinkage strains (Younis, 2016; Zhang et al., 2018).

Conclusively, the overall findings indicate that inclusion of fibres in concrete mixes enhances dimensional stability and mitigates shrinkage cracking which is consistent with previous research on shrinkage control using fibre reinforcement (Mobasher, 2012; Prasannan et al., 2018; Elbehiry et al., 2020).

4.2.8 Water absorption test

For this experimental study, water absorption for both plain (reference) concrete and Mango Fibre Reinforced concrete was determined.

Figure 4.9 presents the effect of varying fibre content and length on water absorption for both plain and Mango Fibre Reinforced concrete at 28 days.

Test results for fibre length (30, 40 and 50 mm) and the corresponding fibre content (0.1%, 0.25%, 1.0% and 1.5%) are presented in Appendix C8. Appendix C8 further shows the following parameters; mean strength, minimum and maximum strength; standard deviation, Coefficient of variation, Correlation coefficients, T-statistics and P-Value for both plain concrete and MFRC.

The following observations and conclusions were drawn; -

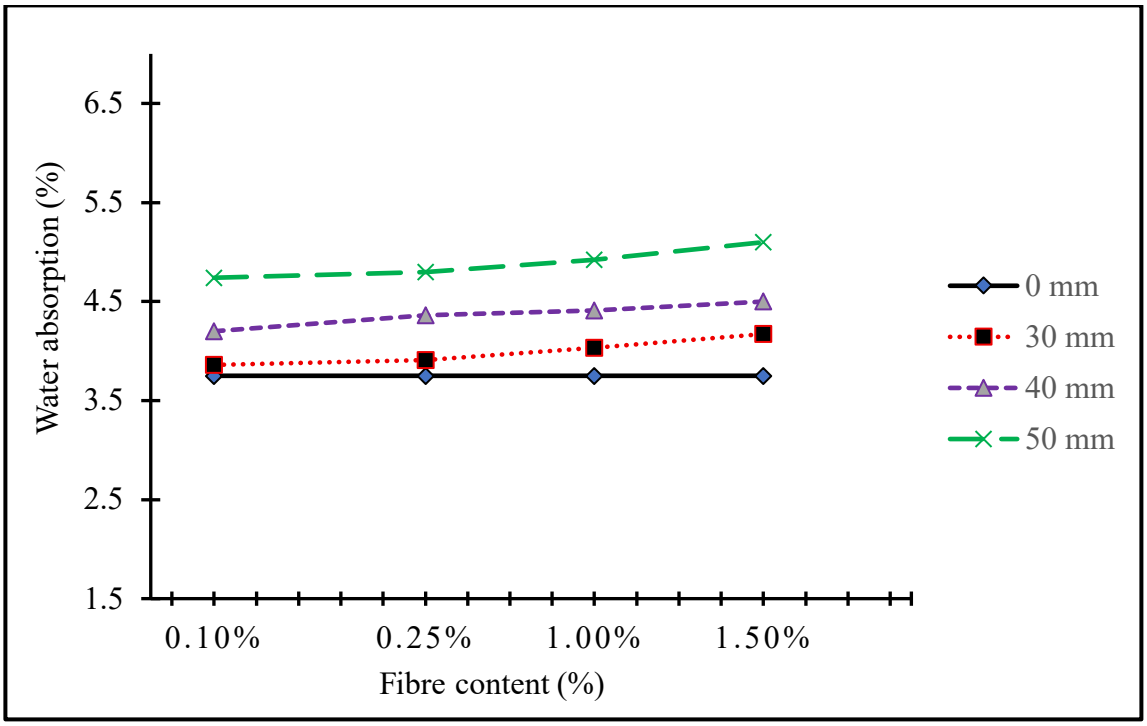

Figure 4.9 Effect of fibre content on water absorption in concrete at 28-days

The water absorption for all fibre contents and lengths was observed to be higher than of the plain concrete. Water absorption in MFRC increased with increasing fibre content and length.

Water absorption increased by 11.2% for 30 mm fibre length and by 20%, for 40 mm fibre length. For 50mm fibre length, water absorption increased by 36% when fibre content was increased from 0.1% to 1.5%.

Finally, there was a strong positive correlation between fibre content and length with water absorption of MFRC for all fibre contents and lengths and, a low coefficient of variation which implied data points were closely clustered around the mean which implied high precision. This indicates that the dataset was consistent with minimal variation.

Additively, the *t*-test *p*-values, however, were considerably above 0.05 ($p \approx 0.95–1.00$), confirming that these differences were not statistically significant at the 95% confidence level.

The water absorption of MFRC was higher than of plain concrete due to natural fibres being hydrophilic in nature (Joseph et Al., 1999; Younis, 2016). Mechanistically, the fibres can absorb and retain water, increasing the overall moisture uptake of the composite. Additionally, at higher fibre contents, voids and microchannels created by fibre clustering or poor dispersion can provide preferential pathways for water penetration, further elevating water absorption.

This behaviour aligns with findings by Zhang et al. (2018) and Eisa et al. (2021), who reported that the inclusion of untreated natural fibres increased the capillary porosity and permeability of the matrix. The interfacial transition zone (ITZ) between fibre and matrix is often weaker and more porous due to incomplete bonding and localized water accumulation during mixing, which contributes to the higher absorption capacity (George et al., 2021).

Despite this, moderate fibre contents have been shown to improve internal curing and delay microcrack formation by redistributing moisture within the matrix (Kim and Park, 2024). None the less, the results are consistent with previous studies on natural fibre composites, confirming that fibre hydrophilicity and distribution play a decisive role in determining water absorption performance (Mobasher, 2012; Elbehiry et al., 2020).

4.2.9 Output from RVE model for MFRC and Plain concrete

4.2.9.1 Consideration for loading

Uniaxial tension and compression loads were applied to simulate tensile and compressive stresses, respectively. Experimental results showed that the uniaxial tensile strengths of plain concrete and mango fibre reinforced concrete (with 1% fibre content and 40 mm fibre length) were 2.70 MPa and 3.40 MPa, respectively. Corresponding compressive strengths were 30.5 MPa for plain concrete and 33.8 MPa for the fibre-reinforced mix.

To simulate the behaviour of mango fibre reinforced concrete (MFRC) and plain concrete, reduced values of uniaxial compressive and tensile strengths were selected and applied to the Representative Volume Element (RVE) as pressure loads. These were incrementally applied at 25%, 50%, 75%, and 100% of the experimentally obtained compressive and tensile strengths to assess progressive loading behaviour.

Failure Criterion applied

Outputs from structural FEA are provided in the form of stresses. Von misses and Maximum principal stress criterion were used for failure prediction when the RVE models for plain concrete (PC) and mango fibre reinforced concrete (MFRC) under Uniaxial Tension and Compression loads. The Von Mises failure criterion was adopted to evaluate the failure mode under uniaxial compressive loading (UCS), while the Maximum Principal Stress criterion was used to assess failure under uniaxial tensile loading (UTS), based on the justification provided in Section 3.8.2 of this research.

Table 4.5 3D RVE Model under compression and tensile loading

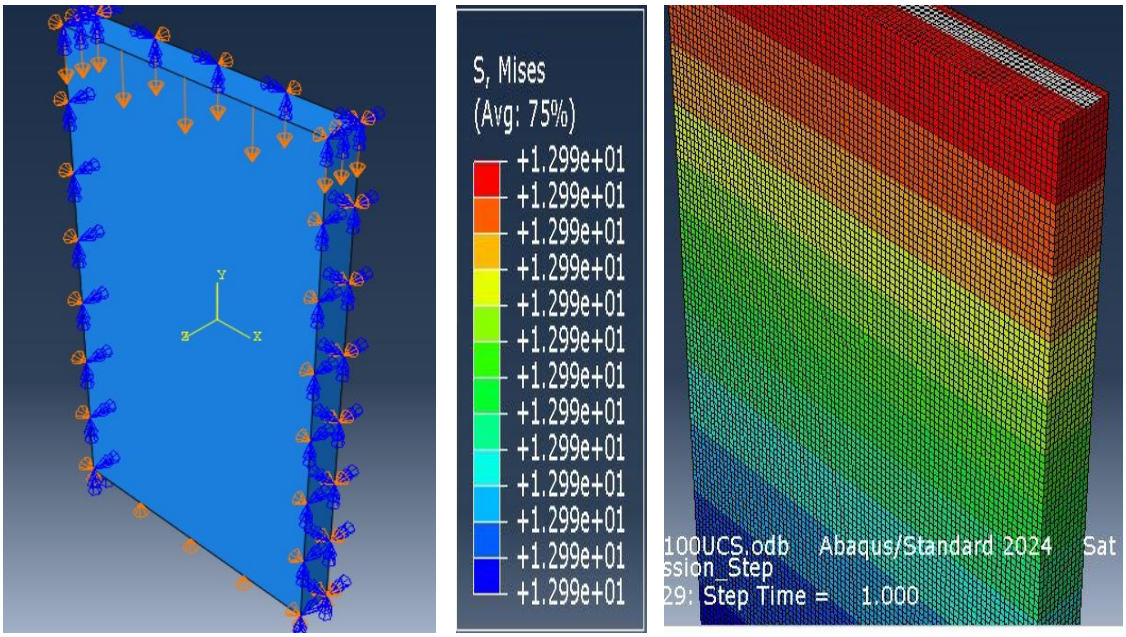

Figure 4.10 UCS application on RVE model for PC

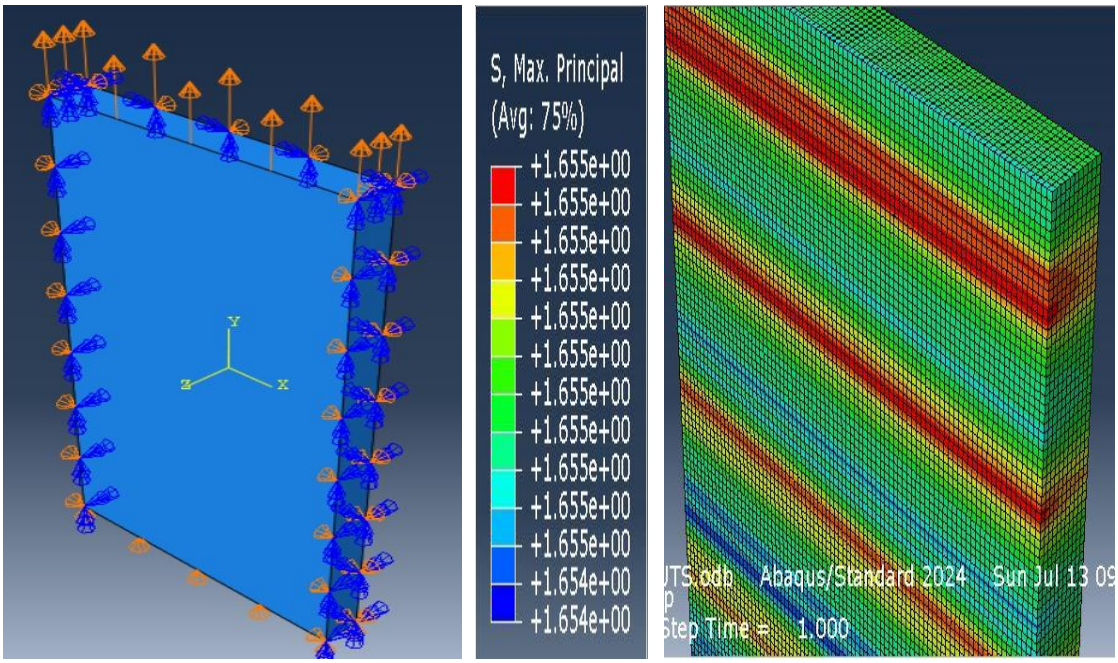

Figure 4.11 UTS application on RVE model for PC

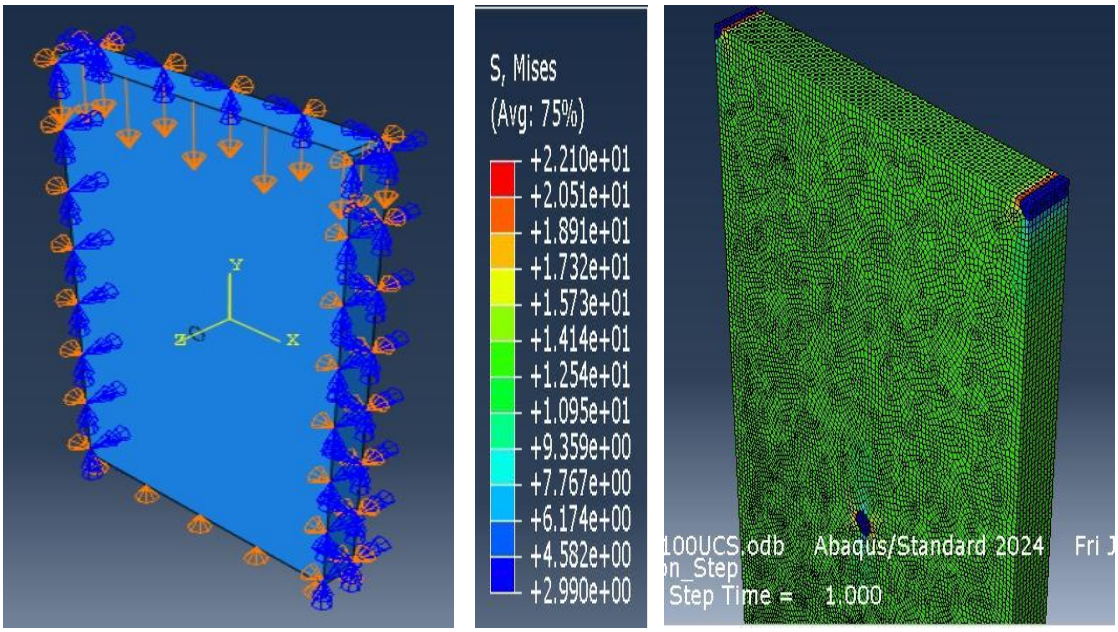

Figure 4.12 UCS application on RVE model for MFRC

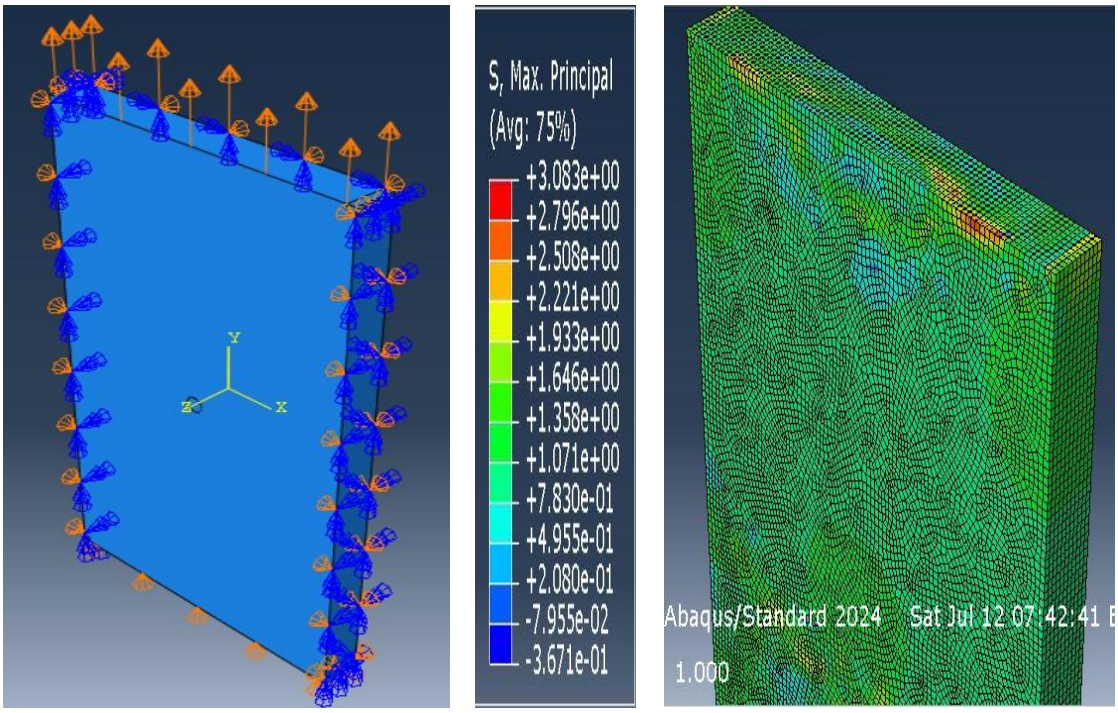

Figure 4.13 UTS application on RVE model for MFRC

Table 4.6 Model deformation under tension and compression loading

TENSILE LOAD								
Experimental results (UTS)	PC	Fibre content – 0.00%					2.70MPa	
	MFRC	Fibre content – 1.0%					3.40MPa	
Proportion of the applied load	25%		50%		75%		100%	
Concrete type	PC	MFRC	PC	MFRC	PC	MFRC	PC	MFRC
Experimental load (MPa)	0.675	0.850	1.350	1.700	2.025	2.550	2.700	3.400
Max. Principal Stresses (MPa)	0.640	0.817	1.279	2.763	1.952	2.480	2.613	3.320
Von Misses (MPa)	2.386	5.860	1.966	8.185	1.729	8.561	1.494	9.808
COMPRESSION LOAD								
Experimental results (UTS)	PC	Fibre content – 0.00%					30.5MPa	
	MFRC	Fibre content – 1.0%					33.8MPa	
Proportion of the applied load	25%		50%		75%		100%	
Concrete type	PC	MFRC	PC	MFRC	PC	MFRC	PC	MFRC
Experimental load (MPa)	7.625	8.450	15.25	16.900	22.875	25.350	30.500	33.800
Von Misses (MPa)	7.510	8.322	15.021	16.658	22.527	25.086	30.042	32.320
Max. Principal Stresses (MPa)	0.000	0.579	0.000	1.158	0.000	1.738	0.000	2.294

Where; - UTS – Uniaxial Tensile Strength and, UCS – Uniaxial Compressive Strength

; - PC – Plain concrete and, MFRC – Mango Fibre Reinforced Concrete

4.2.9.2 Comparison between modelled and experimental outputs under Tension

From table 4.9, maximum principal stress remained below the UTS even at 100% loading which implied no failure for both plain concrete and mango fibre reinforced concrete. Mango fibre reinforced concrete exhibited higher stress capacity than plain concrete at each load case which proved that mango fibres enhance tensile strength of concrete.

4.2.9.3 Comparison between modelled and experimental outputs under Compression

Table 4.9 revealed that, for all load cases, Von Mises stress remained below Uniaxial Compressive Strength (UCS) for both plain concrete and mango fibre reinforced concrete thus, no predicted failure under UCS even at 100% load. Mango fibre reinforced concrete exhibited higher stress capacity than plain concrete at each load case which proved that mango fibres enhance compressive strength of concrete.

4.2.9.4 Discussion of FEM results

The results for plain and mango fibre reinforced concrete subjected under tensile and compressive loading conditions confirmed the role of fibres in bridging and preventing further expansion and propagation of cracks through sharing and redistribution of stresses across the matrix (Mobasher, 2012).

In compression, the MFRC model demonstrated more uniform stress distribution and delayed localization of plastic strain compared to plain concrete, consistent with experimental findings by Elbehiry et al. (2020) and Younis (2016). Under tension, the FEM results revealed lower maximum principal stresses and a gradual stress transfer

across the fibre–matrix interface, validating the fibre-bridging effect described by Mobasher (2012).

To assess model accuracy, the simulated peak stresses and strains were compared with experimental values. The mean deviation between FEM-predicted and experimentally measured compressive strengths was within ±8%, and the tensile strength deviation within ±10%, demonstrating acceptable predictive accuracy for material behaviour ($R^2 \approx 0.92$). These differences can be attributed to assumptions of material homogeneity and perfect fibre–matrix bonding in the numerical model, which may slightly idealize the real physical behaviour.

Overall, the FEM validation confirmed that the numerical model reliably captured the stress redistribution and crack-bridging mechanisms observed experimentally, supporting the mechanical interpretation of fibre-induced improvements in ductility and post-peak behaviour.

4.2.9.5 Validation for FEA results

To validate the RVE finite element model, simulation results were compared with experimental data for both plain concrete (PC) and mango fibre-reinforced concrete (MFRC) under uniaxial compressive and tensile loading. Experimental data were presented with standard deviation error bars to account for material variability and testing uncertainty.

a) Compressive strength

To verify the reliability of the FEM model, its predicted compressive strengths were compared with the experimental results for both plain concrete and MFRC. Figure 4.10 presents this comparison and illustrates how closely the simulated response aligns with the measured laboratory performance.

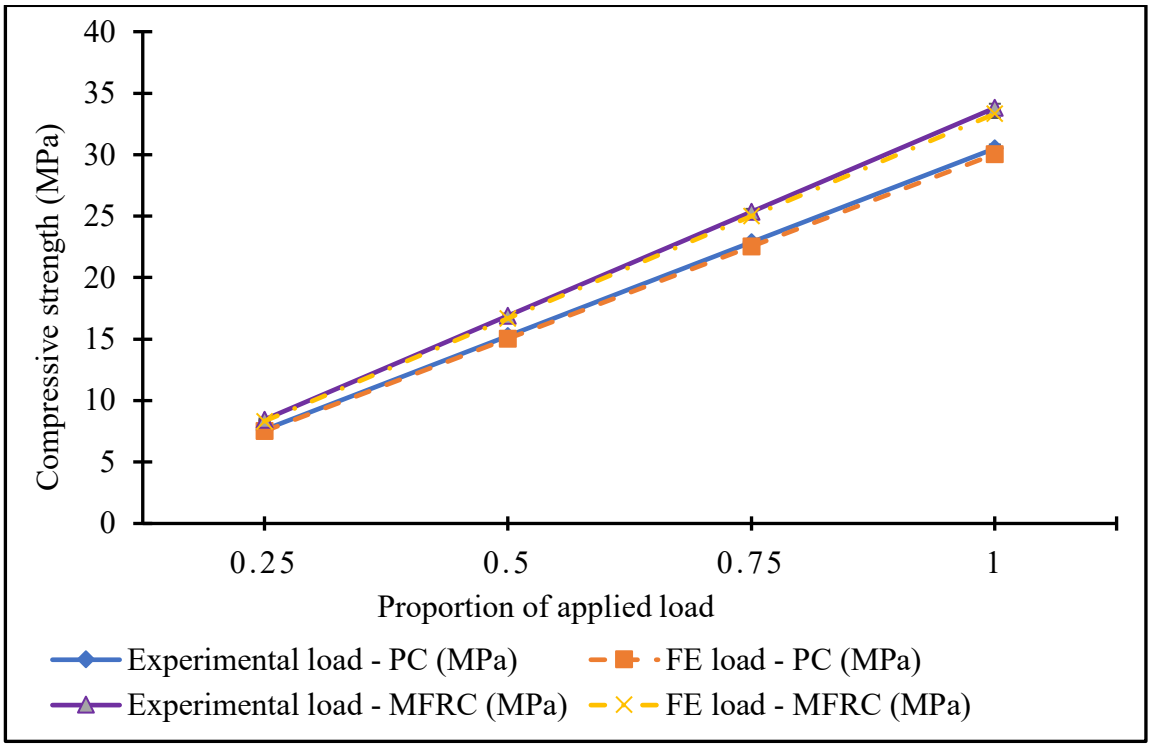

Figure 4.10 Validation graph for compression loading

From Figure 4.10, the Representative Volume Element (RVE) simulations closely matched the average experimental compressive strengths of both plain concrete and mango-fibre-reinforced concrete. The predicted peak stresses fell within the experimental scatter range, demonstrating good agreement between numerical and laboratory results. The MFRC model exhibited delayed failure and increased load-bearing capacity,

consistent with experimental observations, confirming that fibre inclusion enhanced the material's resistance to compressive failure.

A critical evaluation of the FEM results showed that the simulation effectively captured the nonlinear post-peak response and stiffness degradation observed experimentally. Minor deviations in the descending branch of the stress–strain curve were attributed to simplifications in the constitutive material model, such as the assumption of perfect fibre–matrix bonding and isotropic material behaviour. These simplifications slightly idealized the real interfacial mechanics but did not significantly affect global strength prediction. The close alignment between the FEM and experimental curves therefore indicates a high degree of model fidelity and validates the mechanical assumptions adopted in the simulation.

b) Tensile strength

The accuracy of the FEM model under tensile loading was assessed by comparing the simulated tensile strengths with the corresponding experimental results for both plain and mango fibre–reinforced concrete. Figure 4.11 presents this comparison, illustrating how well the numerical tensile response aligns with laboratory observations.

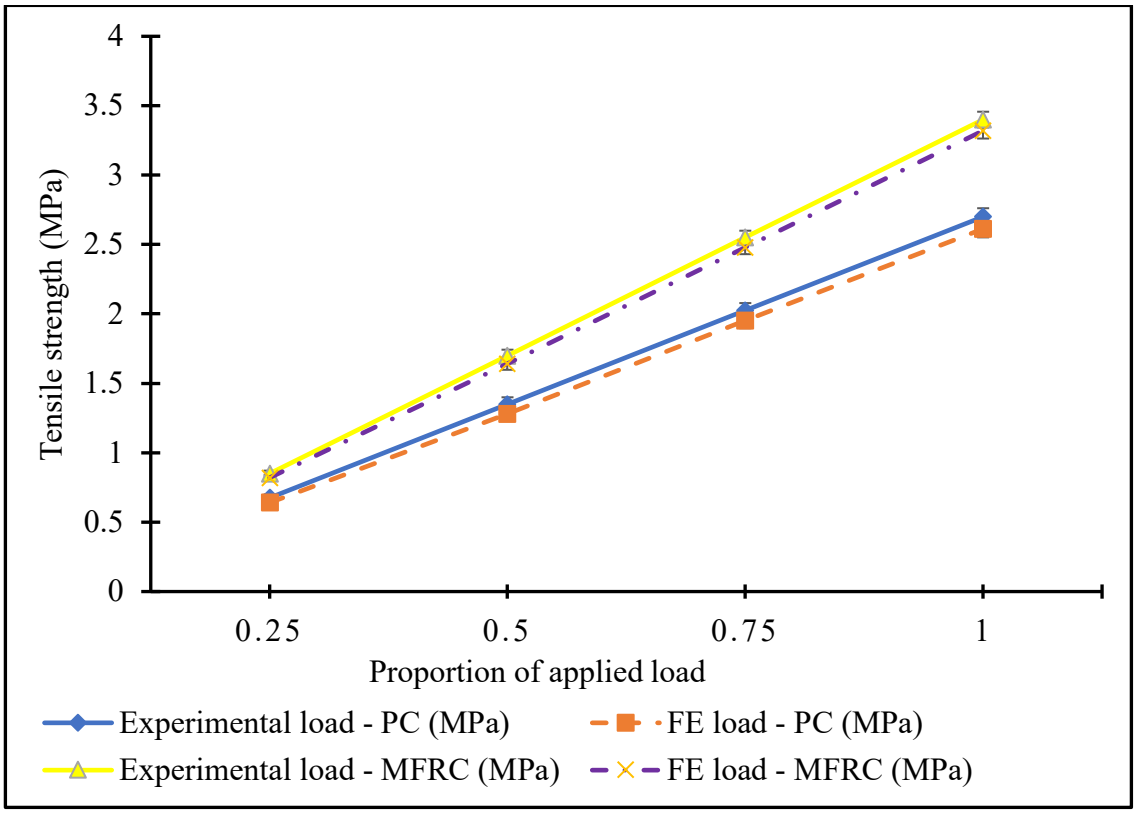

Figure 4.11 Validation graph for tension loading

From Figure 4.11, the RVE model effectively captured the tensile response of both plain concrete and mango-fibre-reinforced concrete. The simulated tensile strengths closely aligned with the experimental mean values, confirming the model's reliability in predicting tensile capacity. The plain concrete model exhibited early brittle failure, while the mango-fibre-reinforced model sustained higher stresses and larger strains owing to the fibre bridging mechanism, which delayed crack propagation and enhanced energy absorption.

A closer evaluation of the simulation indicated that the FEM results not only reproduced the peak tensile strengths but reflected the progressive post-cracking softening observed

experimentally. Minor discrepancies between the numerical and experimental curves were attributed to simplifications in fibre distribution and perfect interfacial bonding assumptions, which idealized the microstructural interactions between fibres and matrix. Nonetheless, the predicted tensile stress–strain trends remained within the experimental scatter range, demonstrating the model's capacity to accurately capture both the initiation and evolution of cracking in fibre-reinforced concrete under tension.

CHAPTER FIVE: CONCLUSIONS AND RECOMMENDATIONS

5.1 Conclusions

In this study, the influence of mango fibres on the structural properties of concrete was investigated through experimental testing and numerical modelling. The mechanical behaviour of Mango Fibre Reinforced Concrete (MFRC) was simulated using the Finite Element Method (FEM) via ABAQUS software.

The independent variables of the study were; - (1) Plain concrete, (2) Mango Fibre Reinforced concrete, (3) Fibre content (0.10%, 0.25%, 1.00% and 1.50%) and; (4) Fibre length (30 mm, 40 mm and 50 mm).

The following conclusions were drawn; -

1. **Properties of mango fibres:** The tensile strength of mango fibres improved by 123.9% upon treatment, breaking elongation was 3.8% and fibre diameter was 66.83 μm. Mango fibre treatment enhanced strength properties of mango fibres. These mechanical and geometrical properties indicate that mango fibres are capable of effectively bridging micro-cracks within concrete, enhancing load transfer and post-cracking toughness. The improvement in fibre strength following treatment highlights the importance of fibre processing in achieving optimal reinforcement efficiency. This contributes to the understanding of natural fibre–matrix interactions and supports the potential use of mango fibres as a sustainable, mechanically effective alternative to conventional synthetic fibres in concrete.

2. **Effect of Mango fibres on structural properties of concrete**

i. **Compressive strength:** Concrete with inclusion of mango fibres exhibited higher compressive strength as compared to plain concrete. The 30 mm fibre length had the highest compressive strength at 1.0% fibre content and for this, compressive strength of concrete increased by 15.74%. For 40 mm and 50 mm fibre lengths, compressive strength increased by 10.8% and 14.43% respectively. These findings indicate that fibre length and content critically influence stress transfer and crack-bridging efficiency in the matrix. The enhanced compressive performance is attributed to the fibres' ability to share load with the surrounding concrete, delay micro-crack propagation, and improve the composite's toughness.

ii. **Flexural strength:** Concrete with inclusion of mango fibres exhibited higher flexural strength as compared to plain concrete. The fibre length that resulted in highest flexural strength was 40 mm at 1.5% fibre content and for this, flexural strength of concrete improved by 54.10%. For 30 and 40mm fibre lengths, flexural strength improved by 50.8% and 44.26% respectively. This trend suggests that fibre length and content strongly influence the material's ability to resist bending stresses by effectively bridging cracks and enhancing post-cracking ductility. The substantial gain in flexural capacity demonstrates the potential of mango fibres to improve tensile load transfer within the concrete matrix, providing both a theoretical understanding of fibre–matrix interaction and practical guidance for designing sustainable fibre-reinforced concrete with optimized mechanical performance.

iii. **Split tensile strength:** Concrete with inclusion of mango fibres exhibited higher split tensile strength as compared to plain concrete. Split tensile strength of concrete increased by 20.6% as fibre content was increased from 0.1% to 1.0% beyond which, a slight reduction was observed. This behaviour can be attributed to the fibres' ability to bridge tensile-induced micro-cracks and enhance stress transfer within the concrete matrix, while higher fibre content likely caused fibre clustering and increased air voids, reducing efficiency. These findings provide insight into the optimal fibre content for maximizing tensile performance and contribute to the theoretical understanding of fibre–matrix interactions in natural fibre-reinforced concrete.

iv. **Drying shrinkage:** Drying shrinkage in MFRC was lesser than that of plain concrete and the effect was more pronounced at higher fibre contents and lengths. For 30 mm fibre length, as fibre content was increased from 0.1% to 1.5%, drying shrinkage reduced to zero and to zero, for 40 mm fibre length, as soon as fibre content was increased to 1.0% and to zero, for 50mm fibre length, as soon as fibre content was increased to 0.25%. This trend demonstrates the effectiveness of mango fibres in restraining volumetric contraction by bridging micro-cracks and distributing internal stresses, highlighting their potential to enhance the dimensional stability of concrete while informing optimal fibre selection for shrinkage control.

v. **Water absorption**: Water absorption in MFRC was higher than that of plain concrete and the effect was more pronounced with increasing fibre content and

length. Water absorption increased by 11.2% for 30 mm fibre length and by 20% for 40 mm fibre length while for 50mm fibre length, by 36% when fibre content was increased from 0.1% to 1.5%. This behaviour is attributed to the hydrophilic nature of mango fibres and the formation of microchannels or voids at higher fibre contents, which facilitate water ingress. These findings highlight a trade-off between mechanical enhancement and moisture susceptibility, providing practical guidance for optimizing fibre content and length to balance structural performance with durability considerations.

3. **Numerical analysis on the mechanical behaviour of MFRC**

   FEM predictions in ABAQUS software revealed that incorporation of fibres enhanced structural properties of concrete. The plain concrete model failed earlier under both tensile and compressive loading, whereas the MFRC model sustained higher stresses and delayed crack propagation. This behaviour highlights the fibres' role in bridging micro-cracks, redistributing stresses, and enhancing post-peak ductility. The FEM results align closely with experimental observations, providing theoretical validation of fibre–matrix interaction mechanisms and confirming the potential of mango fibres as an effective and sustainable reinforcement in concrete.

5.2 Limitations of this research

This study characterized the physical e.g., diameter, fibre length, etc. and mechanical properties e.g., tensile strength, breaking force, breaking elongation, etc. of mango fibres

relevant to concrete performance; however, it did not include an analysis of their chemical composition.

This study was limited to laboratory-based mechanical characterization of mango fibre–reinforced concrete and did not extend to durability assessments or serviceability limit state evaluations. Specifically, chemical resistance tests; such as exposure to sulfate, chloride, or acid attack, were not conducted, and therefore the long-term durability behaviour of mango fibre–reinforced concrete under aggressive environmental conditions remains unverified. In addition, the structural response of mango fibre–reinforced concrete under dynamic or seismic loading conditions was not examined, limiting the generalization of findings to static loading scenarios.

During the finite element analysis (FEA) phase, access to specialized computational resources presented a notable limitation, as extracting simulation results required advanced Python scripts and reference materials such as Barbero's computational micromechanics texts, which were financially demanding for a self-funded researcher. Nevertheless, the study's findings indicate that mango fibres constitute a viable and sustainable alternative for enhancing the structural and durability performance of concrete, with significant implications for policy and industry through the promotion of local fibre utilization, development of supporting standards, and investment in environmentally responsible construction materials.

5.3 Recommendations for future research

There is need for future studies to incorporate detailed chemical and microstructural analyses to provide a more comprehensive understanding of mango fibres as a sustainable reinforcement material for concrete applications. These studies shall establish the influence of the fibres' chemical constituents on hydration reactions and fibre–matrix compatibility of mango fibre reinforced concrete.

Future research should incorporate durability and seismic performance evaluations to comprehensively establish the material's suitability for structural applications. The seismic evaluations shall help establish the structural response of mango fibre–reinforced concrete under dynamic or seismic loading conditions

It is recommended that future research be facilitated through collaborative funding initiatives or institutional licensing of advanced simulation tools to alleviate the cost barriers encountered by self-funded researchers and to enable more comprehensive computational analyses.

REFERENCES

ADEKUNLE (2015) Surface Treatments of Natural Fibres—A Review: Part 1. *Open Journal of Polymer Chemistry*, 05(03), pp. 41–46.

ANAS ET AL. (2022) Fiber Reinforced Concrete: A Review †. *Engineering Proceedings*, 22(1), [Online] Available from: doi.org/10.3390/engproc2022022003.

ANDERSON, T.L. (2006) *0.1. Failure Theories*.

BARBERO, E.J. (2008) Finite element analysis. In: *Finite Element Analysis of Composite Materials*. pp. 51–59.

BARBERO, E.J. (2013) *Finite element analysis of composite materials using abaqus™*.

BS EN 12617-4 (2002) SLOVENSKI STANDARD iTeh STANDARD PREVIEW iTeh STANDARD PREVIEW. *Slovenski Standard*, 2(11), p. 21.

CASAMATTA, D.M. (1986) Synthetic Fiber Reinforced Concrete. *Code News*, No.6(11), pp. 64–67.

DANIEL ET AL. (2002) *Report on Fiber Reinforced Concrete Reported by ACI Committee 544*.

DESAI, C.S. (2012) Application of Finite Element and Constitutive Models. *SOLID, STRUCTURE AND SOIL-STRUCTURE INTERACTION: STATIC, DYNAMIC, CREEP THERMAL ANALYSES*.

DHAWAN ET AL. (2021) Materials Today : Proceedings Evaluation of mechanical properties of concrete manufactured with fly ash , bagasse ash and banana fibre. *Materials Today: Proceedings*, (xxxx), pp. 6–11.

EISA ET AL. (2021) Effect of macro - synthetic fibers on the drying shrinkage performance of rigid pavement. *Innovative Infrastructure Solutions*, (July), [Online] Available from: doi.org/10.1007/s41062-021-00577-y.

ELBEHIRY ET AL. (2020) Case Studies in Construction Materials Performance of concrete beams reinforced using banana fi ber bars. *Case Studies in Construction Materials*, 13, p. e00361.

EMWAMU, S.P. (2020) *Hope fades as Soroti Fruit Factory fails to meet farmer expectations*. [Online] Monitor. Available from : https://www.monitor.co.ug/uganda/news/national/hope-fades-as-soroti-fruit-factory-fails-to- meet-farmer-expectations-1872290.

FERRETTI ET AL. (2021) Representative Volume Element (RVE) Analysis for Mechanical Characterization of Fused Deposition Modeled Components. *polymers*, (3555).

GEORGE ET AL. (2021) Study on the Effect of Fibers on Concrete Shrinkage. *International Research Journal of Engineering and Technology*, 08(07), pp. 498–503.

HABIBI ET AL. (2023) A comprehensive review of natural fibers and their composites: An eco-friendly alternative to conventional materials. *Results in Engineering*, 19(July), p. 101271.

HOSSEINI ET AL (2023) Effect of fiber treatment on physical and mechanical properties of natural fiber-reinforced composites: A review. *Reviews on Advanced Materials Science*, 62(1), [Online] Available from: doi.org/10.1515/rams-2023-0131.

ISABAI ET AL. (2023) Strength Properties of Various Types of Fiber-Reinforced Concrete for Production of Driven Piles. *Buildings*, 13(7), [Online] Available from: doi.org/10.3390/buildings13071733.

JANAMIAN, K. and AGUIAR, J.B. (2023) Introduction to Concrete Technology. *Concrete Materials and Technology*, (March), pp. 1–33.

JANSSON, A. (2008) Fibres in reinforced concrete structures-analysis, experiments and design. *Thesis*, p. 66.

JOHNY, A. (2022) A Review on the Effect of Natural Fibers on Plastic Shrinkage of Concrete. pp. 3209–3215.

JOSEPH ET AL. (1999) *THE USE OF SISAL FIBRE AS REINFORCEMENT IN*.

KARIMAH ET AL. (2021) A comprehensive review on natural fibers: Technological and socio-economical aspects. *Polymers*, 13(24), [Online] Available from: doi.org/10.3390/polym13244280.

KARUBANGA ET AL. (2021) Impact of Addition of Banana Fibres at Varying Fibre Length and Content on Mechanical and Microstructural Properties of Concrete. *Advances in Civil Engineering*, 2021.

KAVITHA ET AL (2017) A review on natural fibres in the concrete. *International Journal of Advanced Engineering and Technology*, 1(1), pp. 4–7.

KIM, S. and PARK, C. (2024) A Review on the Performance of Fibers on Restrained Plastic Shrinkage Cracks. *Building design and construction handbook*.

KNAPPETT, J.A. and CRAIG, R.F. (2012) *Craig ' s Soil Mechanics*. 8th ed.

LAWRENCE ET AL. (2019) *Modeling and Finite Element Analysis*.

LINHUA HUANG ET AL. (2024) The unconfined compressive strength estimation of rocks using a novel hybridization technique based on the regulated Gaussian processor. *Journal of Engineering and Applied Science*, 71(1), pp. 1–22.

MARINA ET AL. (2021) Natural fibers as an alternative to synthetic fibers in reinforcement of geopolymer matrices: A comparative review. *Polymers*, 13(15), [Online] Available from: doi.org/10.3390/polym13152493.

MARKOVSKI ET AL. (2012) Shrinkage strain of concrete - causes and types. [Online] Available from: doi.org/10.14256/JCE.719.2012.

MEGEL, M.E. and HEERMANN, J.A. (1993) Research design. *Plastic Surgical Nursing*, 13(4), pp. 209–210.

MOBASHER, B. (2012) *MECHANICS OF FIBER AND TEXTILE REINFORCED CEMENT*.

MOHANKUMAR ET AL (2021) Extraction of plant based natural fibers – A mini review. *IOP Conference Series: Materials Science and Engineering*, 1145(1), p. 012023.

MOORE, L.O.' (2005) *Investigation of Early Age Tensile Stresses , Shrinkage Strains in Pavements and Standard Drying Shrinkage Tests*.

MUTHUKUMAR, G. (2014) Failure criteria of concrete- A review. *Computers and Concrete*, 14(5), pp. 503–525.

NANJALA, S. (2025) *Soroti Fruits Limited begins processing local mangoes*. [Online] theCooperator. Available from : https://thecooperator.news/soroti-fruits-limited-begins-processing-local-mangoes.

OLIVEIRA ET AL. (2019) The use of natural fibers in repairing and strengthening of cultural heritage buildings. *Materials Today: Proceedings*, 31, pp. S321–S328.

PANDALAI, K.A. V (2018) *COMPOSITE MATERIALS AND STRUCTURES*.

PRAMENDRA KUMAR ET AL. (2018) Analysis of Natural fiber constituents: A Review. *IOP Conference Series: Materials Science and Engineering*, 455(1), [Online] Available from: doi.org/10.1088/1757-899X/455/1/012115.

PRASANNAN ET AL. (2018) COMPARATIVE STUDY OF BANANA AND SISAL FIBRE REINFORCED CONCRETE WITH CONVENTIONAL CONCRETE. *International Journal of Pure and Applied Mathematics*, 118(20), pp. 1757–1765.

RAO, K.M.M. and RAO, K.M. (2007) Extraction and tensile properties of natural fibers: Vakka, date and bamboo. *Composite Structures*, 77(3), pp. 288–295.

RAO, S.S. (2004) • *ISBN: 0750678283 • Publisher: Elsevier Science & Technology Books • Pub. Date: December 2004*.

RASOUL ET AL (2023) A Direct Tensile Strength Testing Method for Concrete from Existing Structures. *CivilEng*, 4(1), pp. 333–344.

REIS ET AL. (2024) Development of Artificial Rock through the Recycling of Construction

Waste and Demolition in Polymeric Materials Development of Artificial Rock Through the Recycling of Construction Waste and Demolition in. (10.20944/preprints202406.0323.v1), [Online] Available from: doi.org/10.20944/preprints202406.0323.v1.

ROESLER ET AL (2006) ACI-Synthetic-2006. *Effect of Synthetic Fibers on Structural Behavior of Concrete Slabs-on-Ground*, M01(103), pp. 3–10.

SHADHEER ET AL (2021) Natural Fibers in Concrete – A Review. *IOP Conference Series: Materials Science and Engineering*, 1055(1), p. 012038.

TINNI ET AL. (2013) *Introduction to concrete pavements*.

UN (2015) The 2030 Agenda for Sustainable Development's 17 Sustainable Development Goals (SDGs). *International Journal of Sustainable Development Goals*.

WAFA, F.F. (2008) Properties and Applications of Fiber Reinforced Concrete. *Innovations and applications of fiber-reinforced concrete*, 2, pp. 49–63.

WHITLOW, R. (1995) *BASIC SOIL MECHANICS*. 3rd ed.

YIMER, T. and GEBRE, A. (2023) Effect of Fiber Treatments on the Mechanical Properties of Sisal Fiber-Reinforced Concrete Composites. *Advances in Civil Engineering*, 2023, [Online] Available from: doi.org/10.1155/2023/2293857.

YOUNIS, K.H. (2016) Mechanical Performance of Concrete Reinforced with Steel Fibres Extracted from Post-Consumer Tyres Mechanical.

ZHANG ET AL. (2018) Fiber-Reinforced Concrete with Application in Civil Engineering. *Advances in Civil Engineering*, 2018, [Online] Available from: doi.org/10.1155/2018/1698905.

APPENDICES

A – Mix design computations

Appendix A.1: Mix Design for Plain concrete (Reference concrete)

For plain concrete
(Reference concrete)

Table 1 Concrete mix design form

Job title C20/25 mix design [Plain concrete]

Stage	Item		Reference or calculation	Values
1	1.1	Characteristic strength	Specified	25 N/mm² at 28 days
				Proportion defective 5 %
	1.2	Standard deviation	Fig 3	8 N/mm² or no data 8 N/mm²
	1.3	Margin	C1 or Specified	(k = 1.64) 1.64 × 8 = 13.12 N/mm²
				N/mm²
	1.4	Target mean strength	C2	✓ 25 + 13.12 = 38.12 N/mm²
	1.5	Cement strength class	Specified	42.5/52.5 ✓
	1.6	Aggregate type: coarse Aggregate type: fine		Crushed/uncrushed ✓ Crushed/uncrushed
	1.7	Free-water/cement ratio	Table 2, Fig 4	0.58
	1.8	*Maximum free-water/cement ratio*	*Specified*	0.5 — Use the lower value: 0.5
2	2.1	Slump or Vebe time	Specified	Slump 30-60 mm or Vebe time – s
	2.2	Maximum aggregate size	Specified	mm
	2.3	Free-water content	Table 3	190 → 190 kg/m³
3	3.1	Cement content	C3	190 ÷ 0.5 = 380 kg/m³
	3.2	*Maximum cement content*	*Specified*	500 kg/m³
	3.3	*Minimum cement content*	*Specified*	330 kg/m³
				use 3.1 if ≤ 3.2 use 3.3 if > 3.1 → 380 kg/m³
	3.4	Modified free-water/cement ratio		
4	4.1	Relative density of aggregate (SSD)		2.6 known/assumed; $\frac{2.62+2.64}{2} = 2.63 \simeq 2.6$
	4.2	Concrete density	Fig 5	2370 kg/m³
	4.3	Total aggregate content	C4	2370 − 380 − 190 = 1800 kg/m³
5	5.1	Grading of fine aggregate	Percentage passing 600 μm sieve	62 %
	5.2	Proportion of fine aggregate	Fig 6	31.5 ≃ 32 %
	5.3	Fine aggregate content	C5	0.32 × 1800 = 576 kg/m³
	5.4	Coarse aggregate content		1800 − 576 = 1224 kg/m³

1 μm = 1/1000 mm
600 μm → 0.6 mm

Quantities	Cement (kg)	Water (kg or litres)	Fine aggregate (kg)	Coarse aggregate (kg) 10 mm	20 mm ✓	40 mm
per m³ (to nearest 5 kg)	380	190	576		1224	
per trial mix of 0.16841 m³	64.0	32.0	97.0		206.1	

Items in italics are optional limiting values that may be specified (see Section 7).
Concrete strength is expressed in the units N/mm². 1 N/mm² = 1 MN/m² = 1 MPa. (N = newton; Pa = pascal.)
The internationally known term 'relative density' used here is synonymous with 'specific gravity,' and is the ratio of the mass of a given volume of substance to the mass of an equal volume of water.
SSD = based on the saturated surface-dry condition.

Computing volume of plain concrete

Cubes (9)

$V_{cu} = 0.15 \times 0.15 \times 0.15 \times 9 = 0.0304\ m^3$

Cylinders, (6)

$V_{cy} = \frac{\pi}{4} \times 0.1^2 \times 0.2 \times 6 = 0.0094\ m^3$

Prisms, (3)

$V_p = 0.4 \times 0.1 \times 0.1 \times 3 = 0.012\ m^3$

Beams (6)

$V_B = 0.75 \times 0.15 \times 0.15 \times 6 = 0.1013\ m^3$

Total volume, $V = V_{cu} + V_{cy} + V_p + V_B$

$= 0.0304 + 0.0094 + 0.012 + 0.1013$

$V = 0.1531\ m^3$

Adding shrinkage factor, $\frac{10}{100} \times 0.1531 = 0.01531\ m^3$

$V_{plain\ concrete} = 0.16841\ m^3$

Appendix A.2: Mix design for Mango Fibre Reinforced Concrete (MFRC)

For FRC

Table 1 Concrete mix design form

Job title C20/25 mix design (FRC)

Stage	Item		Reference or calculation	Values
1	1.1	Characteristic strength	Specified	25 N/mm² at 28 days
				Proportion defective 5 %
	1.2	Standard deviation	Fig 3	8 N/mm² or no data 8 N/mm²
	1.3	Margin	C1 or Specified	(k = 1.64) 1.64 x 8 = 13.12 N/mm²
				N/mm²
	1.4	Target mean strength	C2	25 + 13.12 = 38.12 N/mm²
	1.5	Cement strength class	Specified	✓ 42.5/52.5
	1.6	Aggregate type: coarse Aggregate type: fine		✓ Crushed/uncrushed Crushed/uncrushed ✓
	1.7	Free-water/cement ratio	Table 2, Fig 4	0.58
	1.8	*Maximum free-water/ cement ratio*	*Specified*	0.5 — Use the lower value: 0.5
2	2.1	Slump or Vebe time	Specified	Slump 30-60 mm or Vebe time – s
	2.2	Maximum aggregate size	Specified	mm
	2.3	Free-water content	Table 3	190 kg/m³
3	3.1	Cement content	C3	190 / 0.5 = 380 kg/m³
	3.2	*Maximum cement content*	*Specified*	500 kg/m³
	3.3	*Minimum cement content*	*Specified*	330 kg/m³
			use 3.1 if ≤ 3.2 use 3.3 if > 3.1	380 kg/m³
	3.4	Modified free-water/cement ratio		
4	4.1	Relative density of aggregate (SSD)		2.6 known/assumed
	4.2	Concrete density	Fig 5	2370 kg/m³
	4.3	Total aggregate content	C4	2370 - 380 - 190 = 1800 kg/m³
5	5.1	Grading of fine aggregate	Percentage passing 600 µm sieve	62 %
	5.2	Proportion of fine aggregate	Fig 6	32 %
	5.3	Fine aggregate content	C5	0.32 · 1800 = 576 kg/m³
	5.4	Coarse aggregate content	C5	1800 - 576 = 1224 kg/m³

Quantities	Cement (kg)	Water (kg or litres)	Fine aggregate (kg)	Coarse aggregate (kg) 10 mm	20 mm ✓	40 mm
per m³ (to nearest 5 kg)	380	190	576		1224	
per trial mix of 2.07306 m³	787.8	393.9	1194.1		2537.4	

Items in italics are optional limiting values that may be specified (see Section 7).
Concrete strength is expressed in the units N/mm². 1 N/mm² = 1 MN/ m² = 1 MPa. (N = newton; Pa = pascal.)
The internationally known term 'relative density' used here is synonymous with 'specific gravity' and is the ratio of the mass of a given volume of substance to the mass of an equal volume of water.
SSD = based on the saturated surface-dry condition.

Computing volume of FRConcrete, V_{FRC}

Cubes (108)

$V_{cu} = 0.15 \times 0.15 \times 0.15 \times 108 = 0.3645\ m^3$

Cylinders, (72)

$V_{cy} = \frac{\pi}{4} \times 0.1^2 \times 0.2 \times 72 = 0.1131\ m^3$

Prisms (48)

$V_p = 0.4 \times 0.1 \times 0.1 \times 48 = 0.192\ m^3$

Beams (72)

$V_B = 0.75 \times 0.15 \times 0.15 \times 72 = 1.215 m^3$

Total volume, $V = V_{cu} + V_{cy} + V_p + V_B$

$V = 0.3645 + 0.1131 + 0.192 + 1.215$

$V = 1.8846\ m^3$

Adding shrinkage factor, $\frac{10}{100} \times 1.8846 = 0.18846\ m^3$

$V_{FRC} = 1.8846 + 0.18846 = 2.07306\ m^3$

B – Laboratory test results and certificates

Appendix B.1: Mango fibre test certificate letter

BUSITEMA UNIVERSITY
Pursuing Excellence

P.O. Box 236, Tororo, Uganda
Gen: +256 - 45 444 8838
Fax: +256 - 45 4438517
Email: info@admin.busitema.ac.ug
www.busitema.ac.ug

FACULTY OF ENGINEERING AND TECHNOLOGY
DEPARTMENT OF POLYMER, TEXTILE & INDUSTRIAL ENGINEERING

5th February 2025

Dear Mr. Peter Nagemi
Uganda Christian University

RE: ANALYSIS OF MANGO FIBRE SAMPLES ON ELECTRONIC SINGLE FIBRE STRENGTH TESTER AND SEM

The samples of Treated and Untreated mango fibres were received in the materials and metallurgy laboratory to be analysed on both electronic single fibre strength tester and Scanning Electron Microscope (SEM). During analysis the presented samples were prepared and analysed using both electronic single fibre strength tester with serial number 19139 Model YG003E, Fanyuan, China and TESCAN VEGA 3 SEM equipment with serial number SBU.118-0015, Berno, Czech Republic
The results were sent to Student's email (Peter) for further processing and analysis.
For more information on this contact;

Tumusiime Godias
Senior Technician
0701240292

Copy to;
HoD
Department Technicians

Appendix B.2: Mango fibre test results certificate

BUSITEMA UNIVERSITY
Pursuing excellence

P. O. Box 236 Tororo, Uganda
Gen: +256-45 4448838
Fax: +256-45 4436517
Email: info@adm.busitema.ac.ug
www.Busitema.ac.ug

FACULTY OF ENGINEERING AND TECHNOLOGY
DEPARTMENT OF POLYMER, TEXTILE & INDUSTRIAL ENGINEERING
Section of Materials, Metallurgy and Textile Laboratory

Tuesday 4th February, 2025

Mr. Nagemi Peter,
Uganda Christian University.

RE: TEST RESULTS FOR MANGO SEED FIBRE

Table 1: Physical and Mechanical Properties of Mango Seed Fibres

S/n	Fibre parameter	Equipment/Requirement	Test result, Untreated	Test result, Treated
1.	Stiffness (mm)	FY2027B Stiffness tester	3.2	2.3
2.	Weight (mg)	Precision balance	1.2	0.9
3.	Fibre length (mm)	Steel half meter rule	52	58
4.	Linear density (g/km)	Weight and length	23.08	15.52
5.	Diameter (µm)	Scanning Electron Microscope (TESCAN VEGA 3 SEM)	81.48	66.83
6.	Breaking force (cN)	YG003E Single fibre strength tester	143.68	216.43
7.	Breaking elongation (%)	YG003E Single fibre strength tester	2.3	3.8
8.	Tensile strength (MPa)	Breaking force and diameter	275.57	616.96

Mr. Tumusiime Godias
Senior Technician
Tel: +256701240292
Emails: ttgodias@gmail.com

Appendix B.3: Test certificate for CEM I - 42.5N OPC

TORORO CEMENT LIMITED

(Formaly Tororo Cement Industries Limited)

KAMPALA OFFICE:
P.O. Box 22753 Kampala
Tel: +256 (414) 250065 / 71
+256 (312) 260183 / 184
Fax: +256 (414) 344564
GODOWN 6th Street
Tel: +256 (772) 967836
NAMANVE GODOWN
Tel: +256 (772) 565447

TORORO FACTORY:
P.O. Box 74 , Tororo , Uganda
Tel: +256 (454) 448025 / 75
+256 (352) 512500 (PBX)
Fax: +256 (352) 512517
Email : tcl@tororocement.com
MALABA:
Tel: +256 (454) 442481
Fax: +256 (454) 442278

NEW ROCK BRAND

Week No: 8 **17.02.2025**

CUSTOMER : General
CEMENT TYPE: **PORTLAND CEMENT :CEM I 42.5N**
STANDARD SPECIFICATION: **US EAS 18-1:2017 CEM I 42.5N ;** Equivalence: **EN 197-1**
VESSEL'S NAME: ..... **DESTINATION: GENERAL** .....

CHEMICAL ANALYSIS			
PARAMETER	**SPECIFICATION**	**UNIT**	**RESULTS**
Sulphuric Anhydride (SO_3)	MAX : 3.50	%	**1.70**
Chloride	MAX : 0.10		**0.007**
L.O.I	MAX; 5.0		**1.89**
I.R.	MAX; 5.0		**0.56**
Total alkali Na equalent	NR		**0.567**
Al2O3	MAX: 8.0		**4.37**
Fe2O3	-		**4.21**
CaO	-		**64.17**
MgO	MAX: 3.0		**1.36**
Na2O	-		**0.33**
K2O	-		**0.36**
C3A	-		**4.457**
PHYSICAL TESTS			
TEST	**SPECIFICATION**	**UNIT**	**RESULTS**
Fineness (Blaine) .	NR	M2 / Kg	**345.6**
Setting Time			
(a) Initial	MIN. : 60	Minutes	**150**
(b) Final	MAX : 600	Minutes	**240**
Soundness by Lechatilier	MAX 10.0	mm	**0.0**
Compressive strength			
(a) 48 +/- 1 hour	MIN;10.0	Mpa	**18.95**
(b) 168 +/- 2 hours	NR	Mpa	**31.74**
(c) 672 +/- 4 hours	MIN : 42.5	Mpa	**45.86**

REMARKS: The certificate represents dispatch for Batch No. 17.02.2025.

TORORO CEMENT LTD. P.O.BOX 74 TORORO - UGANDA

Bhadresh Bhatt
Manager (QC & QA)

TORORO CEMENT

PRODUCER & MANUFACTURERS OF :
Portland Cement , galvanised corrugated Iron Sheets,
Ridges & Gutters , Wire nails & Wire Products

Appendix B.4: Compressive strength results

Compressive Strength						
Age of concrete	**7 days**			**28 days**		
	Fibre length			**Fibre length**		
Fibre content	30mm	40mm	50mm	30mm	40mm	50mm
0.1%	27.1	27.5	27.2	30.7	30.8	32.6
0.25%	28.5	29.1	27.6	32.3	32.8	34
1.0%	28.9	33	29.1	35.3	33.8	34.9
1.5%	26.9	32.4	24.9	33	33.3	29.1
Minimum	26.90	27.50	24.90	30.70	30.80	29.10
Maximum	28.90	33.00	29.10	35.30	33.80	34.90
Mean strength	27.85	30.50	27.20	32.83	32.68	32.65
Standard deviation	1.00	2.63	1.74	1.91	1.31	2.55
Coefficient of Variation	0.04	0.09	0.06	0.06	0.04	0.08
Correlation Coefficient	-0.15	0.91	-0.42	0.64	0.74	-0.55
T-statistic	-0.21	3.03	-0.66	1.17	1.54	-0.92
P-value	0.43	0.95	0.29	0.82	0.87	0.23
0.00%	26.7			30.5		

Appendix B.5: Split Tensile strength test results

Split Tensile Strength			
Age of concrete	**28 days**		
	Fibre length		
Fibre content	30mm	40mm	50mm
0.1%	2.8	2.8	2.8
0.25%	2.9	2.9	2.9
1.0%	2.9	3.4	3.1
1.5%	2.7	3.0	2.9
Minimum	2.70	2.50	2.40
Maximum	2.90	3.40	3.10
Mean strength	2.83	2.90	2.83
Standard deviation	0.10	0.39	0.30
Coefficient of Variation	0.03	0.14	0.11
Correlation Coefficient	-0.51	0.73	0.62
T-statistic	-0.84	0.93	0.77
P-value	0.24	0.77	0.74
0.00%	2.7		

Appendix B.6: Flexural strength test results

Flexural Strength			
Age of concrete	**28 days**		
	Fibre length		
Fibre content	30mm	40mm	50mm
0.1%	7.4	7.4	6.6
0.25%	8.0	7.7	7.5

1.0%	8.4	8.5	8.8
1.5%	9.2	9.4	7.5
Minimum	7.40	7.40	6.60
Maximum	9.20	9.40	8.80
Mean strength	8.25	8.25	7.60
Standard deviation	0.75	0.90	0.91
Coefficient of Variation	0.09	0.11	0.12
Correlation Coefficient	0.96	0.99	0.52
T-statistic	4.88	12.07	0.86
P-value	0.98	1.00	0.76
0.00%	6.1		

Appendix B.7: Drying shrinkage test results

Drying shrinkage			
Age of concrete	**28 days**		
	Fibre length		
Fibre content	30mm	40mm	50mm
0.1%	0.70	0.23	0.07
0.25%	0.33	0.07	0.00
1.0%	0.10	0.00	0.00
1.5%	0.00	0.00	0.00
Minimum	0.00	0.00	0.00
Maximum	0.70	0.23	0.07
Mean drying shrinkage	0.28	0.08	0.02
Standard deviation	0.31	0.11	0.04
Coefficient of Variation	1.10	1.45	2.00
Correlation Coefficient	-0.90	-0.81	-0.62

T-statistic	-2.98	-1.96	-1.12
P-value	0.05	0.09	0.19
0.00%	0.97		

Appendix B.8: Water absorption test results

Water absorption			
Age of concrete	**28 days**		
	Fibre length		
Fibre content	30mm	40mm	50mm
0.1%	3.86	4.20	4.74
0.25%	3.91	4.36	4.80
1.0%	4.03	4.41	4.92
1.5%	4.17	4.50	5.10
Minimum	3.86	4.20	4.74
Maximum	4.17	4.50	5.10
Mean strength	3.99	4.37	4.89
Standard deviation	0.14	0.13	0.16
Coefficient of Variation	0.03	0.03	0.03
Correlation Coefficient	0.99	0.90	0.98
T-statistic	11.21	2.90	7.80
P-value	1.00	0.95	0.99
0.00%	3.75		

C – Receipts/ Invoices for material purchase

Appendix C1 – Receipts

e-INVOICE/TAX INVOICE						
Section A: Seller's Details						
TIN:	1000039198					
Legal Name:	LAXICON ENTERPRISES (U) LIMITED					
Trade Name:	LAXICON ENTERPRISES (U) LIMITED					
Address:	215 6 th Street, Industrial Area Nakawa KAMPALA KAMPALA CENTRAL DIVI KAMPALA CENTRAL DIVISION INDUSTRIAL AREA					
Seller's Reference Number:	LX-39834-2022					
Served by:	Laxicon					
Section B: URA Information						
Document Type:	Original					
Issued Date:	12/02/2025					
Time:	13:30:03					
Device Number:	1000039198_01					
Fiscal Document Number:	1241731229383					
Verification Code:	75143296031775867044					
Section C: Buyer's Details						
TIN:	1027418142					
Name:	MR. PETER NAGEMI					
Section D: Goods & Services Details						
No.	**Item**	**Quantity**	**Unit Measure**	**Unit Price**	**Total**	**Tax Category**
1.	Tororo Cement -OPC-CEM I / 42.5 N	10	BG-Bag	45,000	450,000	A
Section E: Tax Details						
Tax Category	**Net Amount**	**Tax Amount**	**Gross Amount**			
A: VAT-Standard (18%)	381,355.93	68,644.07	450,000			
Section F: Summary						
Net Amount:	381,355.93					
Tax Amount:	68,644.07					
Gross Amount:	450,000 Four hundred fifty thousand shillings only.					
Payment Mode						
Cash	450,000					
Total Amount	450,000					
Currency:	UGX					
Number of Items:	1					
Mode:	Online					
Remarks:						
*** END OF e-INVOICE/TAX INVOICE ***						

D – Letters

Appendix D1- Introduction letter from graduate school

KYAMBOGO UNIVERSITY

P. O. BOX 1 KYAMBOGO
Tel: 041 - 4286792 Fax: 256-41-220464
Website :www.kyu.ac.ug Email: drgt@kyu.ac.ug
Directorate of Research and Graduate Training
Office of the Director

APPENDIX 8: INTRODUCTORY LETTER

Date: May 21, 2025

The Managing Director,
Teju Juice Factory
Soroti

The Vice Chancellor,
Busitema University

Dear Sir/Madam,

RE: NAGEMI PETER

This is to introduce to you the above named student **Reg: No 23/U/GMES/0991/PE** pursuing Master of Science in Structural Engineering, Department of Civil and Environmental Engineering, Kyambogo University.

He intends to carry out research on **"The Effect of Mango Fibers on Structural Properties of Concrete: A case of Eastern Uganda"** in partial fulfillment of the requirements of the award of Master of Science in Structural Engineering of Kyambogo University.

The purpose of this letter therefore is to request you to grant him permission to carry out his study in your institution.

Any assistance rendered to him will be highly appreciated.

Yours sincerely,

Prof. Bosco Bua
AG. DIRECTOR

KYAMBOGO UNIVERSITY
★ 21 MAY 2025 ★
DIRECTOR
DIRECTORATE OF RESEARCH AND GRADUATE TRAINING